AGU PUBLICATIONS

Water Resources Research

RESEARCH ARTICLE
10.1002/2016WR019982

This article is a companion to *Fetzer et al.* [2017] doi:10.1002/2016WR019983.

Key Points:
- We review theory and model concepts for evaporation from porous media
- We discuss the underlying assumptions and simplifications of different approaches
- Approaches differ in the description of lateral transport, transport in the air phase of the porous medium, and coupling at the porous medium free flow interface

Correspondence to:
J. Vanderborght,
j.vanderborght@fz-juelich.de

Citation:
Vanderborght, J., T. Fetzer, K. Mosthaf, K. M. Smits, and R. Helmig (2017), Heat and water transport in soils and across the soil-atmosphere interface: 1. Theory and different model concepts, *Water Resour. Res.*, *53*, 1057–1079, doi:10.1002/2016WR019982.

Received 22 OCT 2016
Accepted 5 DEC 2016
Published online 3 FEB 2017

Heat and water transport in soils and across the soil-atmosphere interface: 1. Theory and different model concepts

Jan Vanderborght [1,2], Thomas Fetzer [3], Klaus Mosthaf [4], Kathleen M. Smits [5], and Rainer Helmig [3]

[1]Agrosphere Institute, IBG-3, Forschungszentrum Jülich GmbH, Jülich, Germany, [2]Centre for High-Performance Scientific Computing in Terrestrial Systems, HPSC TerrSys, Geoverbund ABCJ, Forschungszentrum Jülich GmbH, Jülich, Germany, [3]Institute for Modelling Hydraulic and Environmental Systems, Department of Hydromechanics and Modelling of Hydrosystems, University of Stuttgart, Stuttgart, Germany, [4] DTU Environment, Technical University of Denmark, Kgs. Lyngby, Denmark, [5]Department of Civil and Environmental Engineering, Center for Experimental Study of Subsurface Environmental Processes, Colorado Schools of Mines, Golden, Colorado, USA

Abstract Evaporation is an important component of the soil water balance. It is composed of water flow and transport processes in a porous medium that are coupled with heat fluxes and free air flow. This work provides a comprehensive review of model concepts used in different research fields to describe evaporation. Concepts range from nonisothermal two-phase flow, two-component transport in the porous medium that is coupled with one-phase flow, two-component transport in the free air flow to isothermal liquid water flow in the porous medium with upper boundary conditions defined by a potential evaporation flux when available energy and transfer to the free airflow are limiting or by a critical threshold water pressure when soil water availability is limiting. The latter approach corresponds with the classical Richards equation with mixed boundary conditions. We compare the different approaches on a theoretical level by identifying the underlying simplifications that are made for the different compartments of the system: porous medium, free flow and their interface, and by discussing how processes not explicitly considered are parameterized. Simplifications can be grouped into three sets depending on whether lateral variations in vertical fluxes are considered, whether flow and transport in the air phase in the porous medium are considered, and depending on how the interaction at the interface between the free flow and the porous medium is represented. The consequences of the simplifications are illustrated by numerical simulations in an accompanying paper.

1. Introduction

The primary exchanges of heat and water that motivate global and local meteorological conditions occur at the Earth's surface. Many weather and climate phenomena (e.g., monsoons and droughts) are primarily influenced by processes associated with land-atmosphere interactions in which soil moisture and its control on evapotranspiration plays an important role [*Seneviratne et al.*, 2006]. More than half of the Earth's surface is arid or semiarid having little to no vegetative cover [*Katata et al.*, 2007; *Verstraete and Schwartz*, 1991; *Warren*, 1996]. In addition, over 40% of the Earth's terrestrial surface is devoted to agricultural purposes, much of which, due to tillage practices, is bare over a substantial period of the year. Properly describing the water cycle on the basis of heat and water exchanges between the atmosphere and the soil surface is paramount to improving the understanding of water balance conditions in these regions. Despite the importance of these predictions, standard models vary in their ability to predict water fluxes, flow pathways and water distribution. For instance, the fraction of globally averaged evaporation from the soil surface to the total evapotranspiration from the land surface (i.e., including transpiration by the vegetation) varies for different land surface models between 36% and 75% [*Wang and Dickinson*, 2012] with a mean of 58%.

Understanding and controlling evaporation rates from soil is also important at much smaller scales for the water management of cropped soils. For instance, in rain fed agriculture in semiarid regions, where fields are cropped only once every 2 years and water is harvested during the noncropped year, evaporation losses during the noncropped year determine the process or practice efficiency. Evaporation may be reduced in

several ways. First, by tillage, capillaries or fine pores that connect the evaporating soil surface with the water stored deeper in the soil are disrupted, potentially decreasing evaporation fluxes. Nevertheless, tillage may bring deeper wet soil to the soil surface therefore increasing the evaporation losses. In addition, vapor diffusion may be facilitated through the large interaggregate pores in tilled soils. The rougher surface of a tilled soil may also affect reflectivity (albedo) and net radiation [*Potter et al*., 1987] and the vapor transfer between the soil surface and the atmosphere. Tillage-affected soil structure alter the evaporation behavior depending on the weather conditions and may either lead to larger or smaller evaporation losses [*Moret et al*., 2007; *Sillon et al*., 2003; *Unger and Cassel*, 1991]. Another way to reduce evaporation from soil is through a drying concept known as "self-mulching," referring to the development of a dry layer within the soil, which transfers moisture only in the vapor phase [*Li et al*., 2016; *Novak*, 2010]. This naturally formed layer represents an effective way to maintain soil moisture in the subsurface and it can be improved artificially by applying non-natural mulching materials, such as gravel or plastic, to the soil surface in arid/semiarid regions or in various horticultural systems [*Chung and Horton*, 1987; *Modaihsh et al*., 1985; *Tarara and Ham*, 1999; *Yamanaka et al*., 2004]. The physical mechanism is a hygroscopic equilibrium between the soil vapor pressure and the atmospheric humidity, minimizing the evaporation from the mulch [*Fuchs and Hadas*, 2011]. Several experimental studies have been conducted to investigate the effects of mulch properties on soil surface evaporation processes [*Diaz et al*., 2005; *Xie et al*., 2006; *Yuan et al*., 2009]. A negative correlation between evaporation reduction ability and grain size as well as a positive correlation with mulch thickness has been recognized through sensitivity analyses of experimental results. *Or et al*. [2013] reviewed the physical processes that control evaporation processes from porous media and focused on the role of capillary and viscous forces and of diffusive transfers in the porous medium and across the interface between the porous medium and the free flow. This approach allowed them to relate evaporation process to microscopic properties of the porous medium. In simulation models that operate at the continuum scale, these small scale processes and properties must be included in macroscopic properties and constitutive relations between properties, states and fluxes.

Practical and theoretical limitations of modeling efforts at the continuum scale are often magnified at the land-atmosphere interface, where water and energy fluxes are highly dynamic and dramatically influenced by changes in temperature and moisture gradients and direction of flows [*Lehmann et al*., 2012]. The flow and transport behavior at the soil surface is affected by the conditions in the atmosphere (e.g., humidity, temperature, wind velocity, solar radiation) and by the soil thermal and hydraulic properties and states (e.g., thermal and hydraulic conductivity, porosity, capillary pressure, temperature, vapor pressure), all of which are strongly coupled [*Sakai et al*., 2011]. For most subsurface models, the soil surface serves as the upper boundary to the porous medium domain and is characterized using prescribed flux terms that serve as sources and sinks. Similarly, in most atmospheric models, the vadose zone serves as a lower boundary with prescribed fluxes. Such an approach is a simplification of the interaction processes at the common interface of the two flow compartments. Although widely used due to its simplicity and ease of use, such an approach has been shown by both atmospheric and hydrogeological scientists to misrepresent flux conditions, resulting in model prediction errors [*Seager et al*., 2007].

In practice, the Richards equation is the most frequently used conceptual model to describe water movement within the vadose zone, and to simulate water and energy exchanges between the land surface and the atmosphere at the global scale. However, it is mostly used in a form that considers only isothermal liquid water flow but neglects vapor diffusion and air flow in the porous medium and the effects of temperature gradients on flow and transport processes. Although the application of Richards equation has been successful to describe soil water fluxes at various scales [e.g., *Mortensen et al*., 2006; *Nieber and Walter*, 1981; *Schoups et al*., 2005; *Vereecken et al*., 1991], there may arise conditions in which the nonconsidered processes become relevant. The predictive capacities of the Richards equation to evaluate, for instance, surface manipulations that influence air flow, vapor transport and thermal regimes in the porous medium could therefore be questioned. Also for global scale simulations, the consideration of additional processes such as vapor transport in the soil and transport driven by thermal gradients are receiving more attention to reduce the bias in bare soil evaporation predictions that are observed in these models [*Tang and Riley*, 2013b].

Most Richards equation based models assume that soil water flux is one-dimensional (i.e., water flow only occurs vertically), thus neglecting any lateral variations in fluxes within the soil profiles and also at the soil-atmosphere interface. Three-dimensional solutions of the Richards equation have been used to investigate

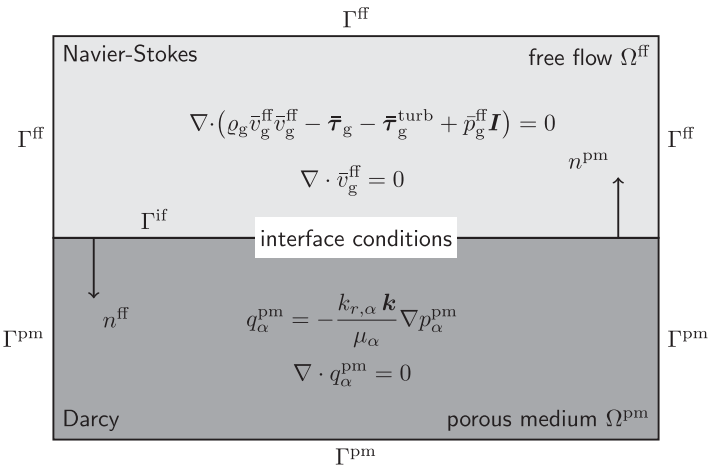

Figure 1. Sketch of the two-domain concept and the notation of the normal vectors (after Mosthaf et al.).

the effect of soil heterogeneity and hence dimensionality on flow and transport processes. However, these simulation studies focused mostly on conditions when flow was directed downward (infiltration). For certain problems of practical relevance, e.g., evaporation from surfaces that are partially covered by mulches or row crops, a multidimensional description of upward flow in the soil is used [*Bristow and Horton*, 1996; *Horton*, 1989]. The few studies that also looked at heterogeneous flow and transport for upward directed flow (evaporation) reported conceptual problems with the definition of the boundary conditions at the soil surface [*Bechtold et al.*, 2012; *Schlüter et al.*, 2012].

Boundary conditions for the Richards equation are determined as a uniform flux boundary condition, which is derived by solving a surface energy balance, as long as a threshold pressure head is not reached. When the soil dries out and the critical pressure head is reached, the boundary condition is switched to a pressure head boundary condition. First, the definition of this critical pressure head is often debated. Second, for a heterogeneous soil surface in which patches of wet soil alternate with dried out areas, the evaporation rate from the wet patches may increase compared to the evaporation from a uniformly wet surface due to lateral exchange processes in the air flow (free flow) or in the porous medium. The effect of lateral exchange processes in the free flow on evaporation leads to the so-called "oasis effect" and has been quantified to evaluate, for instance, the effect of the size of pores [*Assouline et al.*, 2010; *Shahraeeni and Or*, 2012], evaporation pans [*Brutsaert and Yu*, 1968], or ponds and lakes [*Harbeck*, 1962]. Lateral water and heat fluxes in heterogeneous porous media may lead to a larger water loss due to evaporation from a porous medium compared to the water loss from a homogeneous medium [*Lehmann and Or*, 2009; *Shahraeeni and Or*, 2011].

The general objective of this paper is to theoretically compare various model concepts used to describe evaporation processes from soils at the continuum scale. Modeling concepts vary in complexity from fully coupled free flow and porous media flow representations to reduced complexity models such as those using Richards equations. First, we present the modeling concepts for flow and transport in the porous medium (i.e., soil), the free flow (i.e., atmosphere), and the coupling of the porous medium with the free flow (Figure 1). As different scientific communities (soil physics, hydrology, atmospheric sciences and micrometeorology, and fluid mechanics in porous media and in free flow) place different emphasis on the porous medium versus the free flow, oftentimes the coupling is strongly simplified or overlooked. This often leads to inconsistencies in the degree of detail with which processes are described in the porous medium or in the free flow (e.g., 3-D flow in the porous medium coupled with a 1-D transfer resistance to describe the exchange with the free flow) and misunderstandings between communities about the importance of different processes. Therefore, the first objective of this work is to present a comprehensive set of equations that describe all processes in both compartments (free flow and porous medium) and all relevant coupling conditions. This is followed by a discussion of common simplifications that lead to models of reduced complexity. Table 1, provides an overview of the constitutive equations for the two compartments, their interface and potential simplifications. What can be observed immediately from Table 1 is that the variables and parameters used in the various approaches differ significantly.

The second objective is to show the similarities and differences between the different approaches by deriving the variables and parameters based on a theoretical analysis of the comprehensive model. Model simplifications and "fixes" are explained in detail, thus allowing for a full understanding of all approaches and for a classification of the simplifications.

Table 1. Overview of the Equations That Describe Processes in the Porous Medium, the Free Flow, and the Coupling Conditions at the Porous Medium-Free Flow Interface Using Different Degrees of Simplifications

Porous Medium Equations			
Two Component Two Phase	One Component 1.5 Phase (Nonisothermal)	One Component 1.5 Phase (Isothermal)	One Component One Phase (Richards)
Component (Dry Air and Water) and Phase (Gas and Liquid) Equations			
$\sum_{\alpha\in(l,g)} \phi \frac{\partial \rho_\alpha X_\alpha^\kappa S_\alpha}{\partial t} + \nabla \cdot \boldsymbol{F}^\kappa = 0$	$\phi \frac{\partial \rho_g X_g^w S_g}{\partial t} + \phi \frac{\partial \rho_l S_l}{\partial t} + \nabla \cdot \boldsymbol{F}^\kappa = 0$	$\frac{\partial \theta_v}{\partial t} + \frac{\partial \theta_l}{\partial t} =$	$\frac{\partial \theta_l}{\partial t} = \frac{\partial}{\partial z}\left[K_{l,\psi}\frac{\partial \psi}{\partial z} + K_{l,\psi}\right]$
	Equivalent formulation:	$\frac{\partial}{\partial z}\left[\left(K_{l,\psi} + K_{v,\psi}\right)\frac{\partial \psi}{\partial z} + K_{l,\psi}\right]$	
	$\frac{\partial \theta_l}{\partial t} + \frac{\partial \theta_v}{\partial t} = \nabla \cdot \left[\left(\boldsymbol{K}_{l,\psi} + \boldsymbol{K}_{v,\psi}\right)\frac{\sigma(T)}{\sigma(T_{ref})}\nabla\psi|_{Tref} + \boldsymbol{K}_{l,\psi}\boldsymbol{e_z}\right]$		
	$+\nabla \cdot \left(\boldsymbol{K}_{l,T} + \boldsymbol{K}_{v,T}\right)\nabla T$		
$\boldsymbol{F}^\kappa = \sum_{\alpha\in(l,g)} \left(\boldsymbol{q}_\alpha \rho_\alpha X_\alpha^\kappa - D_{\alpha,pm}^\kappa \rho_\alpha \frac{M^\kappa}{M_\alpha}\nabla x_\alpha^\kappa\right)$	$\boldsymbol{F}^w \approx \boldsymbol{q}_l \rho_l - D_{g,pm}^w \left(S_g\right)\nabla \rho_g^w$		
$\boldsymbol{q}_\alpha = -\frac{k_{r\alpha}(S_\alpha)}{\mu_\alpha}\boldsymbol{k}\cdot\nabla(p_\alpha - \rho_\alpha \boldsymbol{g}\cdot\boldsymbol{z})$	$\boldsymbol{q}_l = -\frac{k_{rl}(S_l)}{\mu_l}\boldsymbol{k}\nabla(p_l - \rho_l \boldsymbol{g}\cdot\boldsymbol{z})$		
Heat Equations			
$\sum_{\alpha\in\{l,g\}} \phi \frac{\partial \rho_\alpha u_\alpha S_\alpha}{\partial t} + (1-\phi)\frac{\partial \rho_s c_s T}{\partial t} + \nabla \cdot \boldsymbol{F}_T = 0$			
$\boldsymbol{F}_T = \sum_{\kappa\in\{a,w\}}\sum_{\alpha\in\{l,g\}} \left(\boldsymbol{q}_\alpha \rho_\alpha X_\alpha^\kappa - D_{\alpha,pm}^\kappa \rho_\alpha \frac{M^\kappa}{M_\alpha}\nabla x_\alpha^\kappa\right)h_\alpha^\kappa - \lambda_{T,pm}\nabla T$			
Free Flow Equations			
Mass balance, Reynolds Averaged Navier-Stokes, Component and Energy Balance	1-D Steady State		
$\frac{\partial \rho_g}{\partial t} + \nabla \cdot \left[\rho_g \ \overline{\boldsymbol{v}_g}\right] = 0$			
$\frac{\partial\left(\rho_g \overline{\boldsymbol{v}_g}\right)}{\partial t} + \nabla \cdot \left[\rho_g \ \overline{\boldsymbol{v}_g} \ \overline{\boldsymbol{v}_g} + \overline{p_g}\boldsymbol{I} - \left(\mu_{\boldsymbol{g}}^{\boldsymbol{turb}} + \mu_g\right)\left(\nabla \overline{\boldsymbol{v}_g} + \nabla \overline{\boldsymbol{v}_g}^{\boldsymbol{T}}\right)\right] - \rho_g \boldsymbol{g} = 0$	$\frac{d}{dz}\mu_{\boldsymbol{g}}^{\boldsymbol{turb}}\frac{dv_{gx}}{dz} = 0$		
$\frac{\partial \rho_g \overline{X_g^\kappa}}{\partial t} + \nabla \cdot \left(\rho_g \ \overline{\boldsymbol{v}_g}\,\overline{X_g^\kappa} - \left(D_g^{turb} + D_g^\kappa\right)\rho_g \frac{M^\kappa}{M_g}\nabla \overline{x_g^\kappa}\right) = 0$	$\frac{d}{dz} D_{\boldsymbol{g}}^{\boldsymbol{turb}} \frac{d\rho_g^w}{dz} = 0$		
$\frac{\partial \rho_g \ \overline{u_g}}{\partial t} + \nabla \cdot \left(\rho_g \ \overline{\boldsymbol{v}_g}\,\overline{h_g} - \left(\lambda_{T,g}^{turb} + \lambda_{T,g}\right)\nabla \overline{T} - \sum_{\kappa\in\{a,w\}} h_g^\kappa \left(D_g^{turb} + D_g^{\kappa_i}\right)\rho_g \frac{M^\kappa}{M_g}\nabla \overline{x_g^\kappa}\right) = 0$	$\frac{d}{dz}\lambda_{T,g}^{turb}\frac{dT}{dz} = 0$		

AGU Water Resources Research

10.1002/2016WR019982

AGU Water Resources Research

10.1002/2016WR019982

Table 1. (continued)

Coupling Conditions at the Porous Medium Free Flow Interface			
Two Component Two Phase	1-D Transfer, Aerodynamic Resistances	Semicoupled Using Soil Surface Resistance	Semicoupled Using Threshold
Mechanical Transfer $\left[\boldsymbol{n}\cdot\left(\left\{-\rho_g \boldsymbol{v}_g \boldsymbol{v}_g-\boldsymbol{\tau}_g-\boldsymbol{\tau}_g^{turb}+p_g \boldsymbol{I}\right\}\boldsymbol{n}\right)\right]^{ff}=[p_g]^{pm}$ $\left[\left(\boldsymbol{v}_g+\frac{\sqrt{k_i}}{\alpha_{BJ}\nu_g}\left(\boldsymbol{\tau}_g+\boldsymbol{\tau}_g^{turb}\right)\boldsymbol{n}\right)\cdot\boldsymbol{t}_i\right]^{ff}=0, \quad i\in\{1,\ldots,d-1\}$	$\tau=\rho_g\frac{v_{g,x}(z_{ref})-v_{g,x}(z=0)}{r_M}$ $r_M=\frac{z_{ref}\rho_g ln\left(\frac{z_{ref}}{z_{0m}}\right)}{\mu_g^{turb}(z_{ref})}$		
Component Transfer $\left[x_g^\kappa\right]^{ff}=\left[x_g^\kappa\right]^{pm}, \quad \kappa\in\{a,\ w\}$ $\left[\left(\rho_g \boldsymbol{v}_g X_g^\kappa-\left(D_g+D_g^{turb}\right)\rho_g\frac{M_g^\kappa}{M_g}\nabla x_g^\kappa\right)\cdot\boldsymbol{n}\right]^{ff}=$ $-\left[\left(\rho_g \boldsymbol{q}_g X_g^\kappa-D_{g,pm}^\kappa\rho_g\frac{M_g^\kappa}{M_g}\nabla x_g^\kappa+\rho_l \boldsymbol{q}_l X_l^\kappa-D_{l,pm}^\kappa\rho_l\frac{M_l^\kappa}{M_l}\nabla x_l^\kappa\right)\cdot\boldsymbol{n}\right]^{pm}$	$\frac{\rho_g^w(z=0)-\rho_g^w(z_{ref})}{r_V}=\left[q_l\rho_l-D_{g,eff}^w(S_g)\frac{\partial\rho_g^w}{\partial z}\right]^{pm}$ $r_V\approx r_H=r_M+r_B$	$\frac{\rho_{g,sat}^w\left(z=z_{evap}\right)-\rho_g^w(z_{ref})}{r_V+r_s\left(\theta_{l,top}\right)}=[q_l\rho_l]^{pm}$	*If* $\psi(z=0)>\psi_{crit}$ $\frac{\rho_{g,sat}^w(z=0)-\rho_g^w(z_{ref})}{r_V}=[q_l\rho_l]^{pm}$ *Else* $\psi\ (z=0)=\psi_{crit}$
Heat Transfer $[T]^{ff}=[T]^{pm}$ $\left[\left(\rho_g h_g \boldsymbol{v}_g-\left(\lambda_{T,g}+\lambda_{T,g}^{turb}\right)\nabla T-\sum_{\kappa\in\{a,w\}}h_g^\kappa\left(D_g^\kappa+D_g^{turb}\right)\rho_g\frac{M_g^\kappa}{M}\nabla x_g^\kappa\right)\cdot\boldsymbol{n}\right]^{ff}$ $=R_n-\left[\left(\sum_{\kappa\in\{a,w\}}\sum_{\alpha\in\{l,g\}}\left(\boldsymbol{q}_\alpha\rho_\alpha X_\alpha^\kappa-D_{\alpha,pm}^\kappa\rho_\alpha\frac{M_\alpha^\kappa}{M_\alpha}\nabla x_\alpha^\kappa\right)h_\alpha^\kappa-\lambda_{T,pm}\nabla T\right)\cdot\boldsymbol{n}\right]^{pm}$	$c_a\frac{T(z=0)-T(z_{ref})}{r_H}+h_g^w\frac{\rho_g^w(z=0)-\rho_g^w(z_{ref})}{r_V}-R_n$ $=\left[-h_g^w D_{g,eff}^w(S_g)\frac{\partial\rho_g^w}{\partial z}+h_l^w\rho_l q_l-\lambda_{T,pm}\frac{\partial T}{\partial z}\right]^{pm}$	$c_a\frac{T(z=0)-T(z_{ref})}{r_H}+h_g^w\frac{\rho_{g,sat}^w\left(z=z_{evap}\right)-\rho_g^w(z_{ref})}{r_V+r_s\left(\theta_{l,top}\right)}-R_n$ $=\left[h_l^w\rho_l q_l-\lambda_{T,pm}\frac{\partial T}{\partial z}\right]^{pm}$	*If* $\psi\ (z=0)>\psi_{crit}$ $c_a\frac{T(z=0)-T(z_{ref})}{r_H}+$ $\left(h_g^w-h_l^w\right)\frac{\rho_{g,sat}^w(z=0)-\rho_g^w(z_{ref})}{r_V}-R_n=\left[-\lambda_{T,\,pm}\frac{\partial T}{\partial z}\right]^{pm}$ *Else*: $c_a\frac{T(z=0)-T(z_{ref})}{r_H}-R_n=\left[\left(h_l^w-h_g^w\right)\rho_l q_l-\lambda_{T,\,pm}\frac{\partial T}{\partial z}\right]^{pm}$

In an accompanying paper, the consequences of these simplifications on the predictions of evaporation are investigated for two sets of exemplary simulations.

2. Coupled Heat and Water Flow in Porous Media: Overview of Concepts and Simplifications at the Continuum Scale

In this section, we introduce the model concepts used to describe heat and water fluxes in soils at the continuum scale. From the general balance equations, simplified equations are derived and the assumptions behind these simplifications are discussed. The employed constitutive equations are presented.

2.1. Balance Equations

A full description of water and vapor transport in a porous medium requires a description of flow of the two fluid phases, liquid and gas $\{l, g\}$, and of the transport of the components, water and dry air $\{w, a\}$ in each of the two phases. For simplicity, we consider air as a pseudocomponent consisting of oxygen, nitrogen and other gases except vapor, which is regarded as separate component. A mass balance for each component $\kappa \in \{w, a\}$ is given by:

$$\sum_{\alpha\in(l,g)} \phi \frac{\partial \rho_\alpha X_\alpha^\kappa S_\alpha}{\partial t} + \nabla \cdot \boldsymbol{F}^\kappa = 0 \tag{1}$$

where ϕ is the porosity, which is assumed to be constant, ρ_α is the mass density of phase α [kg m^{-3}], X_α^κ is the mass fraction of component κ in phase α, S_α is the saturation or the volume fraction of the porosity occupied by phase α, $\mathbf{F}^\kappa$ is the mass flux of component κ [kg m^{-2} s^{-1}]. Source and sink terms (e.g., to account for liquid uptake by roots) are not included in the mass balance equations but can be simply added. The component mass flux $\mathbf{F}^\kappa$ is given by:

$$\boldsymbol{F}^\kappa = \sum_{\alpha\in(l,g)} \left(\boldsymbol{q}_\alpha \rho_\alpha X_\alpha^\kappa - D_{\alpha,pm}^\kappa \rho_\alpha \frac{M^\kappa}{\overline{M}_\alpha} \nabla x_\alpha^\kappa \right) \tag{2}$$

where $\boldsymbol{q}_\alpha$ [m s^{-1}] is the volume flux of phase α, $D_{\alpha,\mathrm{pm}}^\kappa(S_\alpha)$ [m^2 s^{-1}] is the effective diffusion coefficient of component κ in phase α in the porous medium, x_α^κ is the molar fraction of κ in α, M^κ is the molar mass of κ and $\overline{M}_\alpha$ is the mole weighted average molar mass of phase α, with $\overline{M}_\alpha = x_\alpha^w M^w + x_\alpha^a M^a$. The effective diffusivity is lower than the diffusivity of κ in phase α alone: D_α^κ due to the tortuosity of the diffusive pathways and the smaller cross-sectional area available for diffusion within the porous medium, which depend both on the phase saturation [*Millington and Quirk*, 1961]. The volume fluxes are calculated with an extended Darcy's law for multiple fluid phases:

$$\boldsymbol{q}_\alpha = -\frac{k_{r\alpha}(S_\alpha)}{\mu_\alpha} \boldsymbol{k} \cdot \nabla(p_\alpha - \rho_\alpha \boldsymbol{g}\boldsymbol{z}) \tag{3}$$

where $k_{r\alpha}(S_\alpha)$ is the relative permeability of phase α at a saturation S_α, $\boldsymbol{k}$ is the intrinsic permeability tensor [m^2], μ_α [Pa s] is the dynamic viscosity of phase α, p_α [Pa] is the phase pressure, $\mathbf{g}$ [m s^{-2}] is the gravitational acceleration vector (directed downward) and $\mathbf{z}$ [m] is the coordinate vector (positive upward). To close the system of equations, supplementary equations need to be specified.

First, the capillary pressure is defined as the pressure difference between the nonwetting and wetting phase: $p_c = p_g - p_l$. According to the Young-Laplace equation capillary pressure depends on the surface tension of the gas-fluid interface, σ [N m^{-1}], and on the curvature of the gas-liquid interfaces, $1/r$ [m^{-1}], which depends on the saturation degree, S_l:

$$p_c = \frac{2\sigma(T)}{r(S_l)} \tag{4}$$

In continuum scale models, functional relations between the saturation degrees of the phases and the capillary pressure: $p_c = f(S_l)$, are used [e.g., *Brooks and Corey*, 1964; *van Genuchten*, 1980]. Using simple pore network models, the form and parameters of relative permeability-saturation functions were linked to the capillary pressure-saturation functions. In the Mualem van-Genuchten model, cylindrical pores are assumed. Assuming other pore geometries, e.g., triangular pores, lead to considerably higher permeabilities under

dry soil conditions [*Diamantopoulos and Durner*, 2015; *Peters and Durner*, 2008; *Tuller and Or*, 2001]. Also, retention functions which describe the dry range of the water retention curve better than the van Genuchten function have been proposed and tested [e.g., *Lu et al.*, 2008] and might be more suited to describe evaporation processes.

Second, the sum of all phase saturations and of all mass fractions equals 1.

Third, a chemical equilibrium of a component between different phases may be assumed. This sets a relation between the mole fraction of air in the liquid phase, x_l^a, and the partial air pressure p_g^a [Pa] in the gas phase using Henry's law. Furthermore, a relation between the vapor pressure and the capillary pressure is given by Kelvin's equation [*Edlefsen and Anderson*, 1943]:

$$p_g^w = p_{g,\mathrm{sat}}^w \exp\left(-\frac{p_c M^w}{\rho_l RT}\right) \tag{5}$$

where $p_{g,\mathrm{sat}}^w$ [Pa] is the temperature-dependent saturated vapor pressure, M^w is the molecular weight of water [kg mol^{-1}], R is the universal gas constant [J mol^{-1} K^{-1}], and T [K] is the absolute temperature. The relation between the capillary pressure and the water vapor pressure only holds for dilute solutions. When the concentration of salts increases, also the osmotic soil water potential must be considered in equation (5) and an additional component equation for salt transport in the liquid phase and chemical equilibrium equations describing salt precipitation and dissolution must be included. We will not consider osmotic effects in the following but refer to [*Nassar and Horton*, 1997, 1999] who describe a model that considers coupled heat, vapor, liquid water, and solute transport. The mole fractions and partial pressures can be directly related to the mass fractions X_α^κ using molar weights and the ideal gas law:

$$\rho_g X_g^w = \rho_g^w = \frac{M^w p_g^w}{RT} = \frac{M^w p_{g,\mathrm{sat}}^w}{RT} \exp\left(-\frac{p_c M^w}{\rho_l RT}\right) \tag{6}$$

where ρ_g^w [kg m^{-3}] is the mass density of the vapor. The mole fraction of vapor in the gas phase can be calculated as:

$$x_g^w = \frac{p_g^w}{p_g} \tag{7}$$

When chemical equilibrium does not hold, extra equations to describe the mass exchange of components between different phases are required [*Benet and Jouanna*, 1982; *Chammari et al.*, 2008; *Nuske et al.*, 2014; *Ouedraogo et al.*, 2013; *Ruiz and Benet*, 2001; *Smits et al.*, 2011; *Trautz et al.*, 2015].

To properly approximate evaporative fluxes, it is important to account for the temperature conditions inside the porous medium. The vapor pressure and density of the air phase are two examples of temperature-dependent state variables. A common assumption is that local thermal equilibrium between the gas, liquid and solid phase exists so that the temperatures in each of the three phases are equal to each other and a single energy balance equation can be used:

$$\sum_{\alpha\in\{l,g\}} \phi \frac{\partial \rho_\alpha u_\alpha S_\alpha}{\partial t} + (1-\phi)\frac{\partial \rho_s c_s T}{\partial t} + \nabla \cdot \boldsymbol{F}_T = 0 \tag{8}$$

where u_α [J kg^{-1}] is the internal energy of phase α, ρ_s [kg m^{-3}] is the mass density of the solid phase, c_s [J kg^{-1} T^{-1}] is the heat capacity of the solid phase, T [K] is the absolute temperature, and $\boldsymbol{F_T}$ [J m^{-2} s^{-1}] is the heat flux. The internal energy is related to the enthalpy, h_α [J kg^{-1}] plus the pressure-volume work:

$$u_\alpha = h_\alpha - \frac{p_\alpha}{\rho_\alpha} \tag{9}$$

The enthalpy of the liquid phase is usually assumed to be independent of composition. The gas phase enthalpy, h_g, is calculated from the mass fractions and component enthalpies, h^κ, of the dry air and water vapor components: $h_g = X_g^a h_g^a + X_g^w h_g^w$. Unlike the enthalpy of liquid water, the enthalpy of vapor also contains the latent heat of evaporation. The heat flux is described by:

$$\boldsymbol{F}_T = \sum_{\kappa\in\{a,w\}} \sum_{\alpha\in\{l,g\}} \left(\boldsymbol{q}_\alpha \rho_\alpha X_\alpha^\kappa - D_{\alpha,pm}^\kappa \rho_\alpha \frac{M^\kappa}{\overline{M}_\alpha} \nabla x_\alpha^\kappa \right) h_\alpha^\kappa - \lambda_{T,pm} \nabla T \tag{10}$$

where $\lambda_{T,pm}$ [J m^{-1} s^{-1} K^{-1}] is the effective thermal conductivity under no mass flow conditions of the mixture of soil grains, liquid, and gaseous phases. Mostly, relations are employed that derive $\lambda_{T,pm}$ from the volumetric liquid phase content. The parameters of these relations are a function of the texture of the porous medium, the organic matter content, and the dry bulk density [*Campbell*, 1985; *Chung and Horton*, 1987; *Cote and Konrad*, 2005, 2009; *de Vries*, 1963; *Lu et al*., 2007; *Tarnawski et al*., 2000]. Under some conditions with high fluid velocities, $\lambda_{T,pm}$ is also a function of the hydromechanical dispersion and heat capacity of the flowing fluid [*Campbell et al*., 1994; *Hopmans et al*., 2002].

2.2. Simplifications and Fixes

In this section, we describe ways to simplify the above derived equations and include additional processes that are not considered in the constitutive equations or simplified equations (e.g., chemical and thermal nonequilibrium and turbulence induced gas phase fluxes in the porous medium).

2.2.1. One Component, "One-and-a-Half" Phase Equation

In this approach, flow of the gas phase is not simulated but diffusive transport of components in the gas phase is still considered. Processes in the gas phase are thus considered "half."

This approach assumes that the pressure in the gas phase, p_g, is uniform and constant with time which results in the independence of the liquid phase pressure from flow in the gas phase. This assumption is justified based on the magnitude of the gas phase viscosity compared to that of the liquid phase (smaller by a factor 50). Therefore, equation (3) is only solved for the liquid phase and gas fluxes can be calculated directly from the change in the liquid phase saturation over time. Second, only the flux of the water component is considered, assuming that the water component flux is not influenced by the dry air concentrations in the two phases. For the liquid phase, this approximation hinges on the fact that the mass fraction of water in the liquid phase is close to one: $X_l^w \approx 1$. For the gas phase, the vapor pressure that is in equilibrium with the liquid phase is calculated from the capillary pressure (equation (5)), which depends only on the liquid phase pressure since the gas phase pressure is assumed to be constant. The vapor concentration is calculated using the ideal gas law (because $X_l^w \approx 1$) (equation (6)) and thus independent of the dry air concentration in the gas phase. Third, it is assumed that advective fluxes of components in the gas phase can be neglected, $\boldsymbol{q_g} \rho_g X_g^w \approx 0$, compared with the diffusive fluxes. Finally, this approach assumes that gradients in the molar volume of the gas phase can be neglected and that the mass density of the liquid phase is constant. As a result of these assumptions, the water component flux equation (equation (2)) reduces to:

$$\boldsymbol{F}^w \approx \boldsymbol{q}_l \rho_l - D_{g,\mathrm{pm}}^w (S_g) \nabla \rho_g^w \tag{11}$$

The mass balance equation for water simplifies to:

$$\phi \frac{\partial \rho_g X_g^w S_g}{\partial t} + \phi \frac{\partial \rho_l S_l}{\partial t} - \nabla \cdot \left[\frac{\rho_l k_{rl}(S_l)}{\mu_l} \boldsymbol{k} \nabla (p_l - \rho_l \boldsymbol{g z}) \right] - \nabla \cdot \left[D_{g,\mathrm{pm}}^w \nabla \rho_g^w \right] = 0 \tag{12}$$

This is the basic equation used by the soil physics community to describe nonisothermal liquid water flow and water vapor transport in soils. However, it is usually expressed in the following form [*Milly*, 1982; *Saito et al*., 2006]:

$$\frac{\partial \theta_l}{\partial t} + \frac{\partial \theta_v}{\partial t} = \nabla \cdot \left[\left(\boldsymbol{K}_{l,\psi} + \boldsymbol{K}_{v,\psi} \right) \frac{\sigma(T)}{\sigma(T_{ref})} \nabla \psi|_{Tref} + \boldsymbol{K}_{l,\psi} \boldsymbol{e_z} \right] + \nabla \cdot \left(\boldsymbol{K}_{l,T} + \boldsymbol{K}_{v,T} \right) \nabla T \tag{13}$$

where $\theta_l = \phi S_l$ is volumetric liquid water content and θ_v the water vapor content expressed in volume of liquid water ($\theta_v = \phi \rho_g^w S_g / \rho_l$), $\boldsymbol{K}_{l,x}$ and $\boldsymbol{K}_{v,x}$ are the hydraulic conductivities for liquid water flow and vapor transport, respectively, $\boldsymbol{K}_{x,\psi}$ [m s^{-1}] and $\boldsymbol{K}_{x,T}$ [m^2 K^{-1} s^{-1}] are the isothermal and thermal hydraulic conductivities, respectively, $\boldsymbol{e_z}$ is the unit coordinate vector in the vertical direction, and $\psi|_{Tref}$ (m) is the pressure head of the liquid phase at the reference temperature T_{ref}. The first term on the right-hand side of equation (13) represents the total water flow due to pressure head gradients under isothermal conditions and due to gravity. Since the pressure head gradients are defined at a reference temperature, a standard relation between θ_l and $\psi|_{Tref}$ can be used. The second term on the right-hand side accounts for the total water fluxes that are generated by a thermal gradient.

In the following section, the relationships between the hydraulic properties $\boldsymbol{K}_{xy}$, the variables θ_v, θ_l, $\psi|_{Tref}$, and T, the fluid properties, and the effective diffusion coefficients and permeability are presented and the equality between equations (12) and (13) elucidated.

The pressure head ψ of the water phase can be defined in terms of the capillary pressure p_c as:

$$p_c = -\psi g \rho_l \tag{14}$$

Assuming a uniform and constant gas phase pressure and liquid phase density, the water pressure gradient can be replaced by the pressure head gradient multiplied by a constant factor $g\rho_l$. Considering equation (4) the spatial gradient of ψ can be written as:

$$\nabla\psi(\theta_l, T) = \frac{\partial\psi}{\partial\theta_l}\bigg|_T \nabla\theta_l + \frac{\partial\psi}{\partial\sigma}\bigg|_{\theta_l} \frac{\partial\sigma}{\partial T}\nabla T \tag{15}$$

or

$$\nabla\psi(\theta_l, T) = \frac{\partial\psi}{\partial\theta_l}\bigg|_T \nabla\theta_l + \frac{\psi}{\sigma}\bigg|_{\theta_l} \frac{\partial\sigma}{\partial T}\nabla T \tag{16}$$

$$\nabla\psi(\theta_l, T) = \frac{\partial\psi}{\partial\theta_l}\bigg|_T \frac{\partial\theta_l}{\partial\psi}\bigg|_{\text{Tref}} \nabla\psi|_{\text{Tref}} + \frac{\psi_{\text{Tref}}}{\sigma(T_{\text{ref}})}\bigg|_{\theta_l} \frac{\partial\sigma}{\partial T}\nabla T \tag{17}$$

$$\nabla\psi(\theta_l, T) = \frac{\sigma(T)}{\sigma(T_{\text{ref}})}\nabla\psi\bigg|_{\text{Tref}} + \frac{\psi_{\text{Tref}}}{\sigma(T_{\text{ref}})}\bigg|_{\theta_l} \frac{\partial\sigma}{\partial T}\nabla T \tag{18}$$

The first term of the right-hand side of equation (16) represents the gradient in pressure head due to a gradient in the volumetric water content under isothermal conditions. Using the relationship between pressure head and volumetric water content at a reference temperature, T_{ref}, this term can be rewritten in terms of a pressure head gradient at a reference temperature (first term of equation (18)). The second term in equation (16) represents the gradient in pressure head due to a temperature gradient at a given volumetric water content θ_l. This term can also be rewritten in terms of a pressure head for a given water content θ_l at a reference temperature (equation (18)).

In a similar vein, the gradient $\nabla\rho_g^w$ can be written as:

$$\nabla\rho_g^w(\psi, T) = \frac{\partial\rho_g^w}{\partial\psi}\bigg|_T \frac{\sigma(T)}{\sigma(T_{\text{ref}})}\nabla\psi\bigg|_{\text{Tref}} + \frac{\partial\rho_g^w}{\partial T}\bigg|_\psi \nabla T \tag{19}$$

Including equations (14), (18), and (19) in equation (12) leads to the following equation:

$$\begin{aligned}\frac{\partial\theta_v}{\partial t} + \frac{\partial\theta_l}{\partial t} = \nabla\cdot\left[\left(\boldsymbol{K}_{l,\psi} + \frac{D_{g,pm}^w(S_g)}{\rho_l}\frac{\partial\rho_g^w}{\partial\psi}\bigg|_T\right)\frac{\sigma(T)}{\sigma(T_{\text{ref}})}\nabla\psi|_{\text{Tref}} + \boldsymbol{K}_{l,\psi}\boldsymbol{e_z}\right] + \\ \nabla\cdot\left[\left(\boldsymbol{K}_{l,\psi}\frac{\psi_{\text{Tref}}}{\sigma(T_{\text{ref}})}\bigg|_{\theta_l}\frac{\partial\sigma}{\partial T} + \frac{D_{g,pm}^w(S_g)}{\rho_l}\frac{\partial\rho_g^w}{\partial T}\bigg|_\psi\right)\nabla T\right]\end{aligned} \tag{20}$$

Using the relation between the vapor density, capillary pressure, and temperature (equation (6)) and defining the saturated vapor density $\rho_{g,sat}^w$ [kg m^{-3}] and the relative humidity of the air $H_r = \rho_g^w/\rho_{g,sat}^w$ it follows from equation (20) that the conductivities in equation (13) are defined as:

$$\boldsymbol{K}_{l,\psi} = \frac{\rho_l g k_{rl}(S_l)}{\mu_l}\boldsymbol{k} \tag{21}$$

$$\boldsymbol{K}_{v,\psi} = \frac{gM_w\rho_{g,sat}^w H_r}{\rho_l RT} D_{g,pm}^w(S_g) \tag{22}$$

$$\boldsymbol{K}_{l,T} = \boldsymbol{K}_{l,\psi}\frac{\psi_{\text{Tref}}}{\sigma(T_{\text{ref}})}\bigg|_{\theta_l}\frac{\partial\sigma}{\partial T} \tag{23}$$

$$\boldsymbol{K}_{v,T} = \frac{H_r}{\rho_l}\frac{\partial \rho^w_{g,sat}}{\partial T} D^w_{g,pm}(S_g) \tag{24}$$

Equation (13) relies on the assumption of local thermal equilibrium. However, the temperature of the air, water, and soil particles may differ due to the difference in thermal properties of these phases and rapid changes of soil surface temperatures. Therefore, it is argued that the temperature gradient in the soil air is often larger than the gradient of the mean temperature over the different phases. The effective diffusion of water vapor in soil may be larger than that of other gases since water vapor may condense and evaporate from capillary held water pockets (i.e., "liquid bridges" or "capillary islands"), thus blocking the diffusive transport of other gases [*Philip and De Vries*, 1957]. These effects have been used to explain observations of enhanced vapor transport compared to Fick's law of diffusion [*Gurr et al*., 1952; *Rollins et al*., 1954; *Taylor and Cavazza*, 1954]. To account for this, $K_{v,T}$ is multiplied by an enhancement factor η [*de Vries*, 1958; *Philip and De Vries*, 1957] described by empirical formulations [e.g., *Campbell*, 1985; *Cass et al*., 1984]. This approach has been widely used and accepted to calculate heat and water flow in soils [e.g., *Hadas*, 1977; *Reshetin and Orlov*, 1998; *Rose*, 1967; *Shepherd and Wiltshire*, 1995; *Sophocleous*, 1979]). However, the validity or need for vapor enhancement has been questioned [*Ho and Webb*, 1998; *Shokri et al*., 2009; *Smits et al*., 2013].

In addition to vapor enhancement, an enhancement of the liquid flow that is induced by thermal gradients has been proposed [*Noborio et al*., 1996; *Saito et al*., 2006]. This enhancement is attributed to the change in surface tension that results from changes in soil water composition (ionic strength, concentration of organic surfactants) with temperature. Thermal enhancement is accounted for by multiplying $K_{l,T}$ (equation (23)) by a nondimensional empirical "gain factor" ranging in value from 0 to 10 [*Nimmo and Miller*, 1986].

In equation (18) and (19), the gradients in the pressure head and vapor mass density were written in terms of gradients in temperature and pressure head at a reference temperature assuming that the change in water content with pressure head, $\frac{\partial \theta_l}{\partial \psi}$, is only a function of the surface tension, σ, and temperature effects were attributed to changes in σ with temperature. But, the relationship between θ_l and ψ also depends on the interaction between the solid and liquid phase (i.e., the contact angle between the liquid-gas surface and the solid phase or solid phase wettability) which may also change with temperature [*Bachmann et al*., 2002]. Therefore, it is important to note that for nonwettable soils temperature effects on solid-liquid phase interactions should be included in the model to predict reduced evaporation from nonwettable soils or reduced water redistribution due to temperature gradients in non wettable soil [*Bachmann et al*., 2001; *Davis et al*., 2014].

2.2.2. Isothermal One Component, "One-and-a-Half" Phase Equation

When water fluxes are considered over a longer period of time (i.e., multiple days), it may be argued that the temporal average of the temperature gradients cancels out due to diurnal variations in temperature. This also results in the temperature gradient driven fluxes canceling out [*Milly*, 1984]. Based on this assumption, the flow equation can be simplified to an isothermal equation and flow due to a temperature gradient (i.e., in equation (13)) can be neglected so that for a 1-D flow process (as routinely assumed in soils), the following equation is obtained:

$$\frac{\partial \theta_v}{\partial t} + \frac{\partial \theta_l}{\partial t} = \frac{\partial}{\partial z}\left[\left(K_{l,\psi} + K_{v,\psi}\right)\frac{\partial \psi}{\partial z} + K_{l,\psi}\right] \tag{25}$$

2.2.3. Isothermal One Component One Phase Equation, Richards Equation

Finally, when vapor transport is neglected, the classical Richards equation is obtained:

$$\frac{\partial \theta_l}{\partial t} = \frac{\partial}{\partial z}\left[K_{l,\psi}\frac{\partial \psi}{\partial z} + K_{l,\psi}\right] \tag{26}$$

3. Flow and Transport Processes in the Atmosphere

In this section, the free flow balance equations are described and then possible simplifications are presented and discussed.

3.1. Balance Equations

In the context of evaporation processes from soils, flow conditions in the free flow are mostly turbulent. Turbulent flow is usually highly irregular with chaotic fluctuations of the local velocity, pressure, concentration and temperature [*Bird et al*., 2007]. These fluctuations are caused by vortices or eddies, which occur over a wide range of length scales. It is possible to simulate all of these phenomena, but it requires the resolution of eddies on all scales and has therefore high computational costs. To reduce these costs, turbulence can be parameterized rather than simulated explicitly. The most commonly used parametrization approach is the so-called Reynolds averaging. The basic assumption is that turbulent fluctuating quantities can be split in a temporal average $\overline{v}$ and a fluctuating part v'. This is called the Reynolds decomposition:

$$v_g=\overline{v}_g+v'_g,\ \ p_g=\overline{p}_g+p'_g,\ \ x_g^\kappa=\overline{x_g^\kappa}+x_g^{\kappa'},\ \ T=\overline{T}+T' \tag{27}$$

where v_g [m s^{-1}] is the gas velocity.

After replacing the instantaneous values in the balance equations by the sum of the average and fluctuating parts, the balance equations are averaged over time. For a more detailed overview on turbulence modeling and the Reynolds averaging procedure, we refer the reader to standard fluid dynamic textbooks [e.g., *Bird et al*., 2007; *Wilcox*, 2006]. The total mass balance for the gas phase is:

$$\frac{\partial \rho_g}{\partial t}+\nabla\cdot\left[\rho_g\ \overline{\boldsymbol{v}_g}\right]=0 \tag{28}$$

The momentum balance is:

$$\frac{\partial\left(\rho_g\overline{\boldsymbol{v}_g}\right)}{\partial t}+\nabla\cdot\left[\rho_g\ \overline{\boldsymbol{v}_g}\ \overline{\boldsymbol{v}_g}+\underbrace{\rho_g\boldsymbol{v}_g'\boldsymbol{v}_g'}_{\substack{\text{turbulent}\\\text{Reynolds}}}+\ \overline{p_g}\boldsymbol{I}-\underbrace{\overline{\boldsymbol{\tau}}_g}_{\substack{\text{stress/}\\\text{stress}}}\right]-\rho_g\boldsymbol{g}=0 \tag{29}$$

The gas phase is considered to act as a Newtonian fluid without dilatation, therefore the shear stress tensor τ_g [kg m^{-1} s^{-2}] solely accounts for the resistance to shear deformation:

$$\boldsymbol{\tau_g}=\mu_g\left(\nabla\overline{\boldsymbol{v}}_g+\nabla\overline{\boldsymbol{v}}_g^{\boldsymbol{T}}\right) \tag{30}$$

where μ_g [kg s^{-1} m^{-1}] is the dynamic viscosity of the gas phase.

The component mass balance is given by:

$$\frac{\partial\rho_g\overline{X_g^\kappa}}{\partial t}+\nabla\cdot\left(\rho_g\ \overline{\boldsymbol{v}_g}\overline{X_g^\kappa}+\underbrace{\rho_g\ \boldsymbol{v}_g'X_g^{\kappa'}}_{\text{turbulent diffusion}}-D_g^\kappa\ \rho_g\frac{M^\kappa}{\overline{M_g}}\nabla\overline{x_g^\kappa}\right)=0 \tag{31}$$

and the energy balance by:

$$\frac{\partial\rho_g\ \overline{u_g}}{\partial t}+\nabla\cdot\left(\rho_g\ \overline{\boldsymbol{v}_g}\overline{h_g}+\underbrace{\rho_g\ \boldsymbol{v}_g'\ h_g'}_{\text{turbulent conduction}}-\lambda_{T,g}\nabla\overline{T}-\sum_{\kappa\in\{a,w\}}h_g^\kappa D_g^\kappa\rho_g\frac{M^\kappa}{\overline{M_g}}\nabla\overline{x_g^\kappa}\right)=0 \tag{32}$$

Multiplication of the turbulent fluctuations in the abovementioned balance equations (e.g., the convective portion of the momentum balance equation) leads to additional terms. Physically speaking, these terms, although originating from the convective portion of the equation, act like additional viscous, diffusive, and conductive forces. Therefore, they are referred to as turbulent stress, turbulent diffusion, or turbulent conduction and require parameterization to properly account for the effects of turbulence. Various parameterizations of different complexity are well-established in literature. The simplest one is based on the Boussinesq assumption [*Boussinesq*, 1877] which states that the Reynolds stress acts completely like a viscous stress so that only one unknown per balance equation remains. These unknowns are called eddy coefficients: eddy viscosity μ_g^{turb} [kg m^{-1} s^{-1}], eddy diffusivity D_g^{turb} [m^2 s^{-1}], and eddy conductivity λ_g^{turb} [W m^{-1} K^{-1}] [*Wilcox*, 2006]. The most fundamental approach for calculating the eddy viscosity is based on the Prandtl mixing length:

$$-\rho_g \boldsymbol{v}_g' \boldsymbol{v}_g' = \boldsymbol{\tau}_g^{\boldsymbol{turb}} = \mu_g^{turb}\left(\nabla \overline{\boldsymbol{v}}_g + \nabla \overline{\boldsymbol{v}}_g^{\boldsymbol{T}}\right)$$
$$\mu_g^{turb} = \rho_g l_{mix}^2 \left|\frac{\partial \overline{v_x}}{\partial z}\right| \tag{33}$$

where $l_{mix} = \kappa z$ is the mixing length [m], κ is the von-Karman constant [–], z is the wall distance [m], and v_x the main velocity component [m s^{-1}]. The dynamic eddy viscosity can be converted to the kinematic eddy viscosity with:

$$\nu_g^{turb} = \frac{\mu_g^{turb}}{\rho_g} = l_{mix}^2 \left|\frac{\partial \overline{v_x}}{\partial z}\right| \tag{34}$$

In this model the kinematic eddy viscosity, ν_g^{turb}, is only a function of the flow and its turbulence, not of the fluid type itself.

In addition to the eddy viscosity, the eddy diffusivity, and conductivity still need to be resolved. The most pragmatic approach is by applying the Reynolds analogy. It assumes that the same mechanisms leading to the eddy viscosity also lead to a higher mixing rate. Then the eddy diffusivity is related to the eddy viscosity by the turbulent Schmidt number:

$$D_g^{\kappa,turb} = \frac{\mu_g^{turb}}{\rho_g Sc^{turb}} \tag{35}$$

In the same way, the eddy conductivity is obtained with the turbulent Prandtl number:

$$\lambda_{T,g}^{turb} = \frac{c_p \mu_g^{turb}}{Pr^{turb}} \tag{36}$$

The turbulent Schmidt and Prandtl numbers are often assumed to be one.

3.2. Simplifications

The solution of the three-dimensional balance equations in the free flow is computationally demanding. To simplify the solution, it is often assumed that the mean wind speed, air temperature, and relative humidity (i.e., vapor content of the air) do not change in the horizontal direction or along the air stream and that their changes over time are slow. This assumption implies that the momentum, vapor, and sensible heat fluxes out of the soil surface are equal to the respective fluxes in the vertical direction in the air stream above the soil surface and do not change with height. This generally applies for a sufficiently large upstream fetch of a homogeneous evaporating surface (no lateral variations in soil water content, soil temperature, evaporation fluxes, and soil surface roughness). It also implies that the vertical component of the air flow is assumed to be zero in both the porous medium and the free flow, which is consistent with the one component "one-and-a-half" phase formulation of the flow and transport process in the porous medium.

When the momentum transfer occurs mainly through turbulent eddies, of which the size increases linearly with height, the eddy viscosity increases linearly with height so that the turbulent shear stress τ_{turb} is given by:

$$\tau_{turb} = \rho_g \kappa v^* z \frac{dv_x}{dz} \tag{37}$$

where v^* [m s^{-1}] is the friction velocity and κ is the von Karman constant ($\approx$0.4). It should be noted that $\rho_g \kappa v^* z$ corresponds with the turbulent viscosity μ_g^{turb} in equation (33). This leads to logarithmic wind profiles that are generally observed in the so-called turbulent or "dynamic" sublayer:

$$v_x(z) = \frac{v^*}{\kappa} ln\left(\frac{z}{z_{0m}}\right) \tag{38}$$

where z_{0m} [m] is the momentum roughness length, which corresponds to the height above the soil surface where extrapolation of equation (38) predicts zero velocity. Similar logarithmic profiles are obtained for the air temperature and humidity. But, because of different interactions at the soil surface, the temperature (z_{0H}) and humidity (z_{0v}) roughness lengths differ from z_{0m}. The relationship between the different roughness lengths and characteristics of the porous medium-free flow interface are discussed in the following section.

4. Heat and Water Fluxes Across the Soil-Atmosphere Interface

The soil-atmosphere interface represents a crucial boundary between the porous medium and the free flow. In this section, the coupling between transport in the atmosphere and the soil is discussed.

4.1. Coupling Conditions

The coupling of the two-phase porous-medium system with turbulent free flow involving the Reynolds-averaged Navier-Stokes equations is based on the model presented in *Mosthaf et al*. [2011] and revised in *Mosthaf et al*. [2014] and *Fetzer et al*. [2016]. It considers continuity of fluxes and a local thermodynamic equilibrium at the interface.

4.1.1. Mechanical Equilibrium

Mechanical equilibrium is defined by the continuity of normal and tangential forces. The normal force acting on the interface from the free flow side is the sum of the inertia, pressure, and viscous forces. The normal force from the porous-medium side of the interface contains only the pressure force, since viscous forces are implicitly accounted for in Darcy's law. Hence, the mechanical equilibrium at the interface in the normal direction can be formulated as:

$$\left[\boldsymbol{n}\cdot\left(\left\{-\rho_g\boldsymbol{v}_g\boldsymbol{v}_g-\tau_g-\tau_g^{\boldsymbol{turb}}+p_g\boldsymbol{I}\right\}\boldsymbol{n}\right)\right]^{ff}=\left[p_g\right]^{pm} \tag{39}$$

The superscripts *ff* and *pm* mark the quantities at the free flow and the porous medium sides of the interface in the sequel. Equation (39) implies that the gas phase pressure may be discontinuous across the interface due to the different model concepts (i.e., Navier-Stokes flow and Darcy flow) in the two domains. Furthermore, in addition to considering the normal forces, the free flow requires a condition for the tangential flow velocity components. When air flows over a porous surface, there is a small macroscopic slip-velocity, which therefore calls the no-slip condition into question. For that purpose, the Beavers-Joseph [*Beavers and Joseph*, 1967] or Beavers-Joseph-Saffman [*Saffman*, 1971] condition can be employed; the latter formulation neglects the comparatively small tangential velocity in the porous medium. The proportionality between the shear stresses τ and the slip velocity at the interface can be described as:

$$\left[\left(\boldsymbol{v}_g-\frac{\sqrt{k_i}}{\alpha_{BJ}\mu_g}\left(\tau_g+\tau_g^{turb}\right)\boldsymbol{n}\right)\cdot\boldsymbol{t}_i\right]^{ff}=0,\qquad i\in\{1,\ldots,d-1\} \tag{40}$$

Here α_{BJ} is the dimensionless Beavers-Joseph coefficient, $\boldsymbol{t}_i$ is a tangential vector, and $k_i=\boldsymbol{t}_i\cdot(k\boldsymbol{t}_i)$ a tangential component of the permeability tensor. The Beavers-Joseph condition was originally developed for flow which is mainly tangential to the porous-medium surface and for laminar single-phase flow in both the free flow and the porous medium. Its applicability for turbulent flow conditions was analyzed by *Hahn et al*. [2002] who concluded that the slip condition for laminar and turbulent flow is the same, because the flow conditions directly at the porous surface can be expected to be laminar (viscous boundary layer) and velocities to be slow.

The influence of the Beavers-Joseph coefficient on the evaporation rate was analyzed in various studies for different flow regimes [*Baber et al*., 2012; *Fetzer et al*., 2016]. For flow parallel to the interface the evaporative fluxes are often dominated by diffusion through the boundary layer normal to the interface [*Haghighi et al*., 2013], whereas the slip velocity promotes transport along the interface.

4.1.2. Chemical Equilibrium

Ideally, chemical equilibrium should be formulated as continuity of the chemical potential. The problem is that the assumption of mechanical equilibrium, as previously discussed, leads to a jump in gas phase pressure across the interface. This jump in gas phase pressure comes along with a jump in vapor pressure across the interface and consequently a jump in chemical potential. Hence, continuity cannot be expressed in terms of chemical potentials. Instead, it is expressed in terms of the continuity of mole fractions in the gas phase.

The continuity of component fluxes is given by:

$$\left[\left(\rho_g \boldsymbol{v}_g X_g^\kappa - \left(D_g + D_g^{turb}\right)\rho_g \frac{M^\kappa}{\overline{M}_g}\nabla x_g^\kappa\right)\cdot \boldsymbol{n}\right]^{ff} = -\left[\left(\rho_g \boldsymbol{q}_g X_g^\kappa - D_{g,pm}^\kappa \rho_g \frac{M^\kappa}{\overline{M}_g}\nabla x_g^\kappa + \rho_l \boldsymbol{q}_l X_l^\kappa - D_{l,pm}^\kappa \rho_l \frac{M^\kappa}{\overline{M}_l}\nabla x_l^\kappa\right)\cdot \boldsymbol{n}\right]^{pm} \tag{41}$$

The minus sign in the flux continuity accounts for the opposed directions of the normal vector of the porous medium and the free flow domain (see Figure 1). When summing up the two components, the continuity of total mass flux is given by:

$$\left[\rho_g \boldsymbol{v}_g \cdot \boldsymbol{n}\right]^{ff} = -\left[\left(\rho_g \boldsymbol{q}_g + \rho_l \boldsymbol{q}_l\right)\cdot \boldsymbol{n}\right]^{pm} \tag{42}$$

4.1.3. Thermal Equilibrium

Thermal equilibrium assumes continuity of temperature at the interface. The free flow temperature is equal to the temperature of the gas phase; in contrast, the porous medium temperature is the temperature of one REV under the assumption of local thermal equilibrium.

The continuity of heat fluxes is given by:

$$\begin{aligned}&\left[\left(\rho_g h_g \boldsymbol{v}_g - \left(\lambda_{T,g} + \lambda_{T,g}^{turb}\right)\nabla T - \sum_{\kappa\in\{a,w\}} h_g^\kappa \left(D_g^\kappa + D_g^{turb}\right)\rho_g \frac{M^\kappa}{\overline{M}}\nabla x_g^\kappa\right)\cdot \boldsymbol{n}\right]^{ff} \\ &= R_n - \left[\left(\sum_{\kappa\in\{a,w\}}\sum_{\alpha\in\{l,g\}}\left(\boldsymbol{q}_\alpha \rho_\alpha X_\alpha^\kappa - D_{\alpha,pm}^\kappa \rho_\alpha \frac{M^\kappa}{\overline{M}_\alpha}\nabla x_\alpha^\kappa\right) h_\alpha^\kappa - \lambda_{T,pm}\nabla T\right)\cdot \boldsymbol{n}\right]^{pm}\end{aligned} \tag{43}$$

The coupling condition for the energy balances may also include the net radiation R_n [J m^{-2} s^{-1}] as an additional energy flux to the porous medium. However, the assumption of thermal equilibrium may be violated in case of fast invasion of water with a different temperature or strong temperature differences between the free flow and porous medium [*Nuske et al*., 2014].

4.2. Simplifications and Fixes

The exchange processes are closely linked to the geometry and the roughness of the interface which is not resolved in the above mentioned simulation models. The effect of this nonresolved geometry or roughness needs to be parameterized in the coupling conditions. In the following section, we discuss several simplifications that are made for coupling processes in the porous medium and the free flow.

4.2.1. Full Turbulence Model and Roughness

For smooth surfaces, the effects of turbulence inside the viscous boundary layer are negligible. Therefore, the eddy coefficients approach zero and are not necessarily required in the coupling conditions.

For smooth surfaces, the roughness elements are covered with a viscous boundary layer, although the flow above the viscous layer may be turbulent. In this case, the roughness influences the profile of the eddy coefficients in the direction normal to the surface and thus the velocity profile and the viscous boundary layer thickness. Still, the coupling occurs in the viscous boundary layer.

For rough surfaces, the height of the roughness elements is larger than the viscous layer thickness and the effects of the roughness and turbulence are important and cannot be neglected [*Fetzer et al*., 2016]. This is accomplished by including the eddy coefficients, which are a function of roughness, in the coupling conditions above. In the section on one-dimensional transfer between the porous medium and the free flow, more details on the effect of roughness on the exchange processes are given.

4.2.2 Coupled One-Dimensional Transfer Between the Soil Surface and Free Flow: Aerodynamic Resistances

When lateral variations in wind, air temperature, and humidity can be neglected, the sensible heat and vapor fluxes can be described as one-dimensional fluxes that are calculated using equivalent transfer resistances and differences in vapor concentrations and temperature that are measured at different heights but at the same horizontal location [e.g., *Monteith and Unsworth*, 1990]:

$$H = c_a \frac{T(z=0) - T(z_{\text{ref}})}{r_H} \tag{44}$$

$$F_w = \frac{\rho_g^w(z=0) - \rho_g^w(z_{\text{ref}})}{r_V} \tag{45}$$

where H [J m^{-2} s^{-1}] is the sensible heat flux, c_a [J m^{-3} K^{-1}] is the volumetric heat capacity of moist air, z_{ref} (m) is a reference height at which wind speed, air temperature and air humidity are measured or defined, F_w [kg m^{-2} s^{-1}] is the water vapor flux, and r_H and r_V [s m^{-1}] are the aerodynamic resistance terms for vertical latent heat and vapor transfer in the air stream. Using a mass and energy balance at the soil surface, the vapor and sensible heat fluxes are linked to the water and vapor fluxes in the soil at the soil surface. The mass balance is given by:

$$F_w = \left[q_l \rho_l - D_{\text{g,eff}}^w(S_g) \frac{\partial \rho_g^w}{\partial z} \right]^{pm} \tag{46}$$

where the first and second terms on the right-hand side are the liquid water and vapor flows toward the soil surface, respectively.

For the energy balance equation at the soil surface, the solar and long wave radiation that is absorbed by and emitted from the soil surface needs to be taken into account. Calling the sum of these radiation terms the net radiation, R_n [J m^{-2} s^{-1}] (where positive radiation terms denote the radiation that is absorbed and negative terms denote the radiation that is emitted), the energy balance at the soil surface is:

$$H + h_g^w F_w - R_n = \left[-h_g^w D_{\text{g,eff}}^w(S_g) \frac{\partial \rho_g^w}{\partial z} + h_l^w \rho_l q_l - \lambda_{T,pm} \frac{\partial T}{\partial z} \right]^{pm} \tag{47}$$

Equations (44–47) link the state variables, i.e., temperature and air vapor concentration, and fluxes at the soil surface with state variables that are defined at the reference height in the air stream. The latter may therefore be considered as Dirichlet boundary conditions for the water and heat fluxes in the coupled soil-air system. This implies that the water and heat fluxes at the soil surface can be derived from these prescribed state variables in the air stream and do not have to be prescribed as flux boundary conditions.

Crucial parameters in equations (44) and (45) are the aerodynamic resistance terms for vertical latent and sensible heat transfer. They are related to the roughness of the soil surface, diffusive transfer in the interfacial viscous or roughness layer, wind velocity and eddy diffusivity in the air stream, and stability of the air above the heated soil surface. In the following discussion, we will consider neutral stability conditions, i.e., the eddy diffusivity is not influenced by buoyancy. We refer the reader to text books on meteorology [e.g., *Brutsaert*, 1982; *Monteith and Unsworth*, 1990; *Shuttleworth*, 2012] for a detailed treatment of buoyancy effects.

In the air stream, a constant shear stress, τ_{turb} [N m^{-2}], with height is assumed. τ_{turb} corresponds to a momentum transfer from the air stream to the soil surface and can be expressed in terms of a resistance equation similar to equations (44) and (45):

$$\tau_{turb} = \rho_g \frac{v_{g,x}(z_{\text{ref}}) - v_{g,x}(z=0)}{r_M} \tag{48}$$

where $v_{g,x}$ [m s^{-1}] is the horizontal air velocity, and r_M [s m^{-1}] is the resistance for momentum transfer between the reference height and the soil surface. r_M is derived from the vertical wind profile in the "logarithmic/dynamic" sublayer above the roughness layer.

Combining equations (37, 38, and 48) leads to the following expression for r_M:

$$r_M = \frac{ln\left(\frac{z}{z_{0m}}\right)}{v^* \kappa} = \frac{\left\{ln\left(\frac{z}{z_{0m}}\right)\right\}^2}{v_{g,x}(z)\kappa^2} \tag{49}$$

The momentum roughness length, z_{0m}, is a function of the kinematic viscosity of air, ν, the friction velocity, v^*, and the height and density of the roughness elements of the soil surface. For rough surfaces, z_{0m} depends only on the roughness of the surface. A prediction of z_{0m} based on the geometry of the surface roughness seems to be very uncertain and *Wieringa* [1993] found that the relationship between z_{0m} and the height of the surface roughness elements, d, may vary between:

$$z_{0m} = \frac{d}{100} \quad and \quad z_{0m} = \frac{d}{5} \tag{50}$$

For a small d or smooth surfaces, a viscous sublayer in which momentum transfer is dominated by kinematic viscosity develops. In such a case, the velocity profiles and z_{0m} depend on v^* and ν:

$$z_{0m} = 0.135 \frac{\nu}{v^*} \tag{51}$$

Whether a surface is rough or (hydrodynamically) smooth depends on the roughness Reynolds number, z_{0+} which is defined as:

$$z_{0+} = \frac{v^* z_{0m}}{\nu} \tag{52}$$

When $z_{0+} > 2$, the surface is considered to be rough whereas z_{0+} equals 0.135 for flat surfaces. It should be noted that when z_{0m} is defined by $d/30$, the following well-known relation for a wind speed profile above a rough surface is obtained [*White*, 1991]:

$$v_x(z) = \frac{v^*}{\kappa} \ln\left(\frac{z}{d}\right) + 8.5 v^* \tag{53}$$

For smooth surfaces, the following relation is obtained:

$$v_x(z) = \frac{v^*}{\kappa} \ln\left(\frac{z v^*}{\nu}\right) + 5.0 v^* \tag{54}$$

The transfer of water vapor and sensible heat in the logarithmic/dynamic sublayer is also caused by turbulence and eddy diffusivity, which according to the Reynolds analogy may be considered equivalent to the eddy viscosity. Therefore, a close relation between the transfer resistances for momentum, sensible heat and vapor transfer may be assumed. Yet, these resistances differ from each other because of the different transfer mechanisms in the viscous or roughness layer. The kinematic air viscosity differs from the molecular diffusion of water and heat. Also, the roughness of a bluff surface has a different effect on momentum transfer than on transfer of a scalar quantity like vapor or sensible heat. For rough surfaces, momentum transfer can be considered more effective or influential than vapor or heat transfer. Therefore, the resistance for heat/vapor transfer is larger than that for momentum transfer. As a consequence, an additional boundary resistance, r_B [s m^{-1}] must be considered when relating the transfer resistances for vapor and sensible heat transfer to the momentum transfer:

$$r_V \approx r_H = r_M + r_B \tag{55}$$

The larger resistance results in a larger gradient of vapor and temperature across the viscous or roughness layer; the vapor and heat roughness lengths z_{0v} and z_{0H} are therefore smaller than z_{0m}. The similar transfer through the logarithmic/dynamic layer allows for the transfer resistance for vapor and heat transport to be described using an equation similar to equation (49)]:

$$r_{V,H} = \frac{ln\left(\frac{z}{z_{0v,H}}\right)}{v^* \kappa} = \frac{\left\{ln\left(\frac{z}{z_{0v,H}}\right)\right\}^2}{v_{g,x}(z)\kappa^2} \tag{56}$$

This equation may be rewritten in terms of r_m and r_B as:

$$r_{V,H} = r_M + r_B = \frac{ln\left[\frac{z}{z_{0v,H}}\right]}{\kappa v^*} = \frac{ln\left[\frac{z}{z_{0m}}\right]}{\kappa v^*} + \frac{ln\left[\frac{z_{0m}}{z_{0v,H}}\right]}{\kappa v^*} = \frac{ln\left[\frac{z}{z_{0m}}\right]^2}{\kappa^2 v_{g,x}(z)} + \frac{ln\left[\frac{z}{z_{0m}}\right] ln\left[\frac{z_{0m}}{z_{0v,H}}\right]}{\kappa^2 v_{g,x}(z)} \tag{57}$$

A number of equations that relate $z_{0v,H}$ with z_{0m} and v^* have been proposed [see, e.g., *Yang et al.*, 2008]. *Brutsaert* [1982] developed the following relation between z_{0m} and $z_{0v,H}$:

$$\frac{z_{0v,H}}{z_{0m}} = 7.4 \exp\left[-2.46\left(\frac{v^* z_{0m}}{\nu}\right)^{0.25}\right] = 7.4 \exp\left[-2.46\left(\frac{k v_{g,x}(z) z_{0m}}{ln\left(\frac{z}{z_{0m}}\right)\nu}\right)^{0.25}\right] \tag{58}$$

In Figure 2, the calculated resistances using equations (49), (50), (57), and (58) for different surface roughness lengths, d and two wind velocities, $v_{g,x}$, at 2 m height above the soil surface are shown. According to these calculations, the total resistance (r_H) decreases with increasing roughness. This can be attributed to the decreasing transfer resistance in the logarithmic/dynamic sublayer with increasing roughness of the soil surface. However, the difference between transfer resistance for momentum transfer, r_M, and heat/vapor transfer, $r_{V,H}$ (i.e., $r_{B,}$) increases with increasing roughness. For heat/vapor transfer, the effect of larger turbulent diffusivity in the logarithmic/dynamic layer above a rougher soil surface is counteracted by a longer diffusive pathway through a thicker roughness layer. As a consequence, the decrease of the resistance for heat/vapor transfer with increasing surface roughness is less prevalent than the decrease of momentum transfer resistance (Figure 2).

It should be noted that the transfer resistances described above are based on the assumption of a bluff surface with a no-slip boundary condition. As described before, slip conditions may apply at the surface of a porous medium, which can be accounted for by Beavers-Joseph interface boundary conditions. One way to represent these effects is to define a displacement height, similar to what is used to describe momentum, heat, and vapor transfer between vegetated surfaces and the atmosphere. However, this displacement height should be negative. We are at this moment, not aware of any studies that specify such displacement heights for air flow over rough dry porous media.

4.2.3 Semicoupled Porous Medium and Free Flow Using Potential Evaporation Rates and Soil Surface Resistances for Drying Porous Medium

In the sections above, we described how water flow and heat transport in the porous medium and the free flow are coupled at the interface. However, this coupling is often relaxed by specifying or defining state variables a priori at the interface. When the vapor pressure at the interface is defined to be the saturated vapor pressure, the water flux from the interface into the free flow is:

$$F_{\mathrm{w,pot}} = \frac{\rho^{w}_{g,sat}(z=0) - \rho^{w}_{g}(z_{ref})}{r_V} \tag{59}$$

where $F_{w,pot}$ is the so-called potential evaporation, which is calculated without considering the porous medium. It represents the "demand" for water by the atmosphere and can be used as a flux boundary condition in the porous medium as long as the flow in the porous medium can "supply" the demand. The saturated vapor concentration at the soil surface depends on the soil surface temperature, which is derived from solving the surface energy balance (equation (47)).

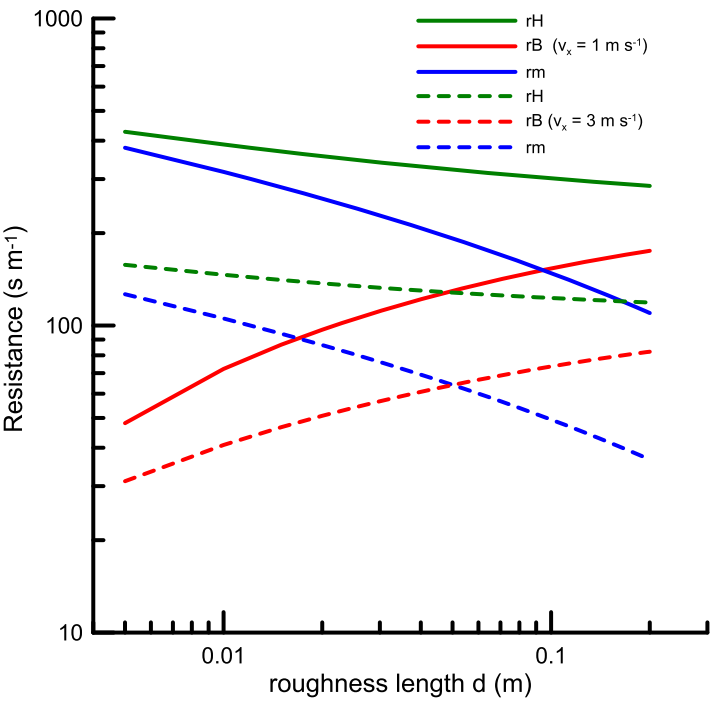

Figure 2. Aerodynamic resistances for sensible heat (and vapor) (r_H) and momentum transfer (r_m) through the boundary layer as function of the surface roughness length, d, for two different wind speeds, $v_{g,x}$ at 2 m height. *rB* represents the additional resistance for heat transfer compared with momentum transfer.

An additional soil transfer resistance, r_s [s m^{-1}] was introduced to account for a reduction in evaporation when the soil surface dries out and the vapor pressure becomes smaller than the saturated vapor pressure:

$$F_w = \frac{\rho^{w}_{g,sat}\left(z=z_{evap}\right) - \rho^{w}_{g}(z_{ref})}{r_V + r_s\left(\theta_{l,top}\right)} = \beta\left(\theta_{l,top}\right) F_{w,pot} \tag{60}$$

where z_{evap} is the depth where evaporation takes place (i.e.,

where air is assumed to be saturated with vapor) and $\theta_{l,top}$ is the water content of the "top soil layer". However, neither z_{evap} nor the thickness of the top soil layer are explicitly defined or simulated. The soil transfer resistance, r_s, is a function of the water content in the top soil layer whereas r_v depends on the free flow conditions. Water transport in the porous medium and into the atmosphere is hence semicoupled in this approach. The β factor represents the ratio of the aerodynamic resistance to the sum of the soil and aerodynamic resistance. This approach is often used in large-scale simulation models to describe the reduction of evaporation from drying bare soil compared with the potential evaporation from wet soil [*Tang and Riley*, 2013a].

Kondo et al. [1990], *Mahfouf and Noilhan* [1991], and *Vandegriend and Owe* [1994] used a soil transfer resistance term that increases with decreasing surface soil water content to account for the additional resistance for diffusive vapor transfer when the evaporative surface recedes into the soil profile and *Tang and Riley* [2013a] derived a model for the soil transfer resistance based on the vapor diffusivity and liquid water hydraulic conductivity. Experimentally derived soil transfer resistances were smaller than expected, considering the depth of the evaporation surface and the vapor diffusion coefficient. The smaller resistances were attributed to turbulent eddies that propagate into the porous medium and generate upward and downward movement of air and hence an extra opportunity for mixing with incoming air in the upper soil layer [*Farrell et al*., 1966; *Ishihara et al*., 1992; *Kimball and Lemon*, 1971; *Scotter and Raats*, 1969]. It should be noted that *Assouline et al*. [2013] found that the evaporation flux calculated using Ficks' Law and the depth of the evaporation front (i.e., z_{evap}) underestimated the evaporation rate; however turbulent mixing was not recognized in this case as a potentially relevant process. Additional turbulent mixing leads to an additional dispersive flux of gases in the upper soil layer and has been shown to be of importance for the flux of vapor and trace gases from soil [*Baldocchi and Meyers*, 1991; *Maier et al*., 2012; *Poulsen and Moldrup*, 2006] and soil covered with mulches [*Fuchs and Hadas*, 2011]. The parameterization of this additional mixing due to turbulence in the top soil is not well known and debated.

A second reason for a decrease in evaporation rate from a drying surface is the spatial variation of the vapor pressure at the soil surface at the microscopic scale. When the lateral distance between evaporating water surfaces in pores at the soil surface becomes too large, the reduction of the evaporating water surface when the soil surface dries out cannot be compensated by an increased lateral diffusion of vapor through the viscous or roughness layer [*Haghighi et al*., 2013; *Shahraeeni et al*., 2012; *Suzuki and Maeda*, 1968]. In this case, vapor transfer through the viscous or roughness layer rather than vapor transfer within the porous medium is the limiting factor. If this effect is also accounted for by an additional resistance term, experimental results of *Shahraeeni et al*. [2012] suggest that this resistance term increases with decreasing surface soil water content, that it is larger in soils with larger pores, and that the ratio of this resistance term to the resistance for vapor transport from a saturated soil surface increases with increasing wind velocity. It should be noted that a similar relation with wind speed is observed for the ratio of r_B/r_M (see Figure 2).

Soil transfer resistances have been introduced in soil evaporation models. However, using an additional transfer resistance in a model that explicitly considers diffusive vapor transfer in the soil surface layer [e.g., *Saito et al*., 2006] leads to a double counting of the transfer resistance through the soil surface layer and therefore a too strong and rapid decrease in the actual evaporation rate from the soil surface.

4.2.4 Threshold Formulation of Boundary Conditions

In this approach, water transfer between the porous medium and the free flow is either fully controlled by free flow conditions or by water transport in the porous medium. When the free flow controls the transfer, the potential evaporation is used as a flux boundary condition for water flow in the porous medium. When the porous medium controls the flux, a constant water pressure or water content at the surface of the porous medium is defined and the water flux toward the soil surface is calculated by solving the flow equations in the porous medium for a Dirichlet boundary condition. This approach is used in soil models that solve the Richards equation, e.g., Hydrus 1-D [*Simunek et al*., 2008]. There are no exact guidelines to define the critical pressure head, ψ_{crit}, which is kept constant at the porous medium surface. As a rule of thumb, ψ_{crit} should correspond with a pressure head for which the hydraulic conductivity and capacity of the porous medium ($d\theta/d\psi$) become very small so that a smaller ψ_{crit} would hardly influence simulated water contents and water fluxes toward the soil surface. As will be shown in some simulation examples in the accompanying paper, simulated water fluxes are not so sensitive to the exact choice of this critical pressure head.

5. Summary and Conclusions

This work presented an overview of concepts with different complexity that can be used to describe the transfer of water and energy from a porous medium into free flow. We identified how the different approaches are related and which simplifications are used. The most comprehensive description of processes considered multidimensional flow of liquid and gas phases and transport of dry air and water components in the porous medium that was coupled consistently acknowledging mechanical, chemical and thermal equilibrium at the interface to a free flow in the gas phase and transport of vapor and heat above the porous medium. Since the direction of the free flow is generally different from the main direction of the flow and transport processes in the porous medium, this comprehensive approach implies a multidimensional description of the flow and transport processes.

However, for homogeneous soil surfaces of a sufficiently large fetch, lateral variations in state variables in the free flow become very small. This leads to a first simplification from a multidimensional to a one-dimensional description of the flow and transport processes in which only the vertical components of flow and transport (in the porous medium) are considered and the vertical components of the gas flow in both the porous medium and the free flow are neglected. This implies that in the porous medium transport in the gas phase happens by diffusion only (i.e., air flow is neglected). This assumption allows to couple the water and heat fluxes in the porous medium and in the free flow at the porous medium interface using transfer resistances that calculate fluxes from states at the soil/free flow interface and at a defined height in the free flow.

A second simplification assumes that vapor transport in the porous medium can be neglected leading to the one component one phase or so-called Richards equation. This simplification decouples water from heat fluxes in the porous medium. At the porous-medium free flow interface, the heat balance equation is solved to determine the water flux at the interface. This balance is solved assuming that the vapor concentration at the soil surface is equal to the saturated vapor concentration so that the heat balance equation is in fact decoupled from the water flow equation in the porous medium. The water fluxes that are derived from this heat balance apply therefore only when the soil surface is sufficiently wet.

The third set of simplifications is related to the description of the interactions or the coupling of the water flow in the porous medium, the interface heat balance, and the evaporation from the interface. In a first approach the transfer between the porous medium and free flow is described by threshold boundary conditions that use prescribed fluxes derived from a surface energy balance until a critical threshold water pressure head is reached at the porous medium surface. This so-called Richards equation with threshold boundary conditions is widely used in soil water balance models. During periods when the pressure head at the surface equals the critical pressure head, the dynamics of the evaporation fluxes are completely defined by the hydraulic properties of the porous medium and the water distribution in the porous medium but are decoupled from the dynamics of the evaporative forcing: radiation, free flow velocity, relative humidity and temperature. A second approach, which is often used in large-scale simulation models, combines the diurnal dynamics of the evaporation of a wet surface with a soil surface resistance depending on the soil water content and represents a semicoupling between the dynamics of the evaporative forcing and the flow process in the porous medium.

Finally, there are processes that are not represented or resolved in the comprehensive process description that we presented. These processes are parameterized in the vapor transport description in the porous medium and in the transfer resistances for momentum, heat and vapor transfer between the porous medium and the free flow. Processes like turbulent diffusion and enhancement of thermal vapor diffusion by thermal nonequilibrium within the porous medium are parameterized in the vapor transport. Nonequilibria (thermal and chemical) can be included in the models by adding additional equations that describe the rate with which an equilibrium is reached, typically first-order rates [*Smits et al*., 2011]. The rate coefficients are in essence additional empirical parameters that need to be estimated, for example by inverse modeling. Since the surface roughness is not represented in the continuum equations, the effect of roughness on the exchange processes needs to be parameterized in the transfer resistances. Because the small scale mechanisms that control the exchange processes at a rough interface differ for momentum vs heat and vapor exchanges, the parameterizations of the respective transfer resistances differ. However, these parameterizations have been derived mainly for bluff surfaces. Therefore, the effect of vertical (turbulent pumping) and

lateral gas flow in the surface layer of the porous medium, which may be important in highly porous mulches, aggregated soils, and dry soils, is not accounted for.

Based on this summary, we conclude that the description of evaporation processes in systems where an important lateral variation in fluxes and states can be expected would require a multidimensional representation of the processes in both the porous medium and the free flow. Although this seems at first sight trivial, it is in fact not generally applied. For instance, several studies that investigated the effect of soil heterogeneity on soil water fluxes use a multidimensional description of the flow process in the porous medium but describe the transfer from the soil surface into the atmosphere using transfer resistances that presume laterally homogeneous state variables in the free flow.

The consideration of the vapor transport in the porous medium and its parameterization due to nonrepresented processes or its indirect representation in transfer resistances between the porous medium and the free flow is another important difference between the presented model concepts. Under which conditions these differences lead to important differences in simulated evaporation needs to be further investigated.

These conclusions are the starting point of accompanying paper in which we will evaluate the impact of lateral variability and the representation of vapor transport in the porous medium on evaporation simulations.

Acknowledgments
The authors would like to acknowledge the German Science Foundation, DFG. This work is a contribution of the DFG research unit "Multi-Scale Interfaces in Unsaturated Soil" (MUSIS; FOR 1083) and the DFG International Research Training Group NUPUS and the National Science Foundation (NSF EAR-1447533). The authors would like to thank the editor and the anonymous reviewers for their insightful comments and suggestions that have contributed to improve this paper.

References

Assouline, S., K. Narkis, and D. Or (2010), Evaporation from partially covered water surfaces, *Water Resour. Res.*, *46*, W10539, doi:10.1029/2010WR009121.

Assouline, S., S. W. Tyler, J. S. Selker, I. Lunati, C. W. Higgins, and M. B. Parlange (2013), Evaporation from a shallow water table: Diurnal dynamics of water and heat at the surface of drying sand, *Water Resour. Res.*, *49*, 4022–4034, doi:10.1002/wrcr.20293.

Baber, K., K. Mosthaf, B. Flemisch, R. Helmig, S. Müthing, and B. Wohlmuth (2012), Numerical scheme for coupling two-phase compositional porous-media flow and one-phase compositional free flow, *IMA J. Appl. Math.*, *77*(6), 887–909, doi:10.1093/imamat/hxs048.

Bachmann, J., R. Horton, and R. R. van der Ploeg (2001), Isothermal and nonisothermal evaporation from four sandy soils of different water repellency, *Soil Sci. Soc. Am. J.*, *65*(6), 1599–1607, doi:10.2136/sssaj2001.1599.

Bachmann, J., R. Horton, S. A. Grant, and R. R. van der Ploeg (2002), Temperature dependence of water retention curves for wettable and water-repellent soils, *Soil Sci. Soc. Am. J.*, *66*(1), 44–52, doi:10.2136/sssaj2002.4400.

Baldocchi, D. D., and T. P. Meyers (1991), Trace gas-exchange above the floor of a deciduous forest. 1: Evaporation and co2 efflux, *J. Geophys. Res.*, *96*(D4), 7271–7285, doi:10.1029/91JD00269.

Beavers, G. S., and D. D. Joseph (1967), Boundary conditions at a naturally permeable wall, *J. Fluid Mech.*, *30*, 197–207, doi:10.1017/s0022112067001375.

Bechtold, M., J. Vanderborght, L. Weihermuller, M. Herbst, T. Gunther, O. Ippisch, R. Kasteel, and H. Vereecken (2012), Upward transport in a three-dimensional heterogeneous laboratory soil under evaporation conditions, *Vadose Zone J.*, *11*(2), doi:10.2136/vzj2011.0066.

Benet, J. C., and P. Jouanna (1982), Phenomenological relation of phase-change of water in a porous-medium: Experimental-verification and measurement of the phenomenological coefficient, *Int. J. Heat Mass Transfer*, *25*(11), 1747–1754, doi:10.1016/0017-9310(82)90154-5.

Bird, R. B., W. E. Stewart, and E. N. Lightfoot (2007), *Transport Phenomena*, 905 pp., Wiley, New York.

Boussinesq, J. (1877), Essai sur la théorie des eaux courantes, *Mem. Acad. Sci.*, *23*(1), 1–680.

Bristow, K. L., and R. Horton (1996), Modeling the impact of partial surface mulch on soil heat and water flow, *Theor. Appl. Climatol.*, *54*(1–2), 85–98, doi:10.1007/BF00863561.

Brooks, R. H., and A. T. Corey (1964), Hydraulic properties of porous media, *Rep.*, Colorado State University, Fort Collins, Colo, No. 3.

Brutsaert, W. (1982), *Evaporation into the Atmosphere. Theory, History, and Applications*, 299 pp., D. Reidel Publ., Dordrecht, Netherlands.

Brutsaert, W., and S. L. Yu (1968), Mass transfer aspects of pan evaporation, *J. Appl. Meteorol.*, *7*(4), 563–566, doi:10.1175/1520-0450(1968)007<0563:MTAOPE>2.0.CO;2.

Campbell, G. S. (1985), *Soil Physics With Basic*, Elsevier, New York.

Campbell, G. S., J. D. Jungbauer, W. R. Bidlake, and R. D. Hungerford (1994), Predicting the effect of temperature on soil thermal-conductivity, *Soil Sci.*, *158*(5), 307–313.

Cass, A., G. S. Campbell, and T. L. Jones (1984), Enhancement of thermal water-vapor diffusion in soil, *Soil Sci. Soc. Am. J.*, *48*(1), 25–32, doi:10.2136/sssaj1984.03615995004800010005x.

Chammari, A., B. Naon, F. Cherblanc, B. Cousin, and J. C. Benet (2008), Interpreting the drying kinetics of a soil using a macroscopic thermodynamic nonequilibrium of water between the liquid and vapor phase, *Dry. Technol.*, *26*(7), 836–843, doi:10.1080/07373930802135998.

Chung, S. O., and R. Horton (1987), Soil heat and water-flow with a partial surface mulch, *Water Resour. Res.*, *23*(12), 2175–2186, doi:10.1029/WR023i012p02175.

Côté, J., and J. M. Konrad (2005), A generalized thermal conductivity model for soils and construction materials, *Can. Geotech. J.*, *42*(2), 443–458, doi:10.1139/t04-106.

Côté, J., and J. M. Konrad (2009), Assessment of structure effects on the thermal conductivity of two-phase porous geomaterials, *Int. J. Heat Mass Transfer*, *52*(3–4), 796–804, doi:10.1016/j.ijheatmasstransfer.2008.07.037.

Davis, D. D., R. Horton, J. L. Heitman, and T. S. Ren (2014), An experimental study of coupled heat and water transfer in wettable and artificially hydrophobized soils, *Soil Sci. Soc. Am. J.*, *78*(1), 125–132, doi:10.2136/sssaj2013.05.0182.

de Vries, D. A. (1958), Simultaneous transfer of heat and moisture in porous media, *Trans. AGU*, *39*(5), 909–916, doi:10.1029/TR039i005p00909.

de Vries, D. A. (1963), Thermal properties of soils, in *Physics of Plant Environment*, edited by W. R. V. Wijk, pp. 210–235, North Holland Publ. Co., Amsterdam.

Diamantopoulos, E., and W. Durner (2015), Closed-form model for hydraulic properties based on angular pores with lognormal size distribution, *Vadose Zone J.*, *14*(2), doi:10.2136/vzj2014.07.0096.

Diaz, F., C. C. Jimenez, and M. Tejedor (2005), Influence of the thickness and grain size of tephra mulch on soil water evaporation, *Agric. Water Manage.*, *74*(1), 47–55, doi:10.1016/j.agwat.2004.10.011.
Edlefsen, N. E., and A. B. C. Anderson (1943), Thermodynamics of soil moisture, *Hilgardia*, *15*(2), 31–298, doi:10.3733/hilg.v15n02p031
Farrell, D. A., E. L. Greacen, and C. G. Gurr (1966), Vapor transfer in soil due to air turbulence, *Soil Sci.*, *102*(5), 305–313, doi:10.1097/00010694-196611000-00005.
Fetzer, T., K. M. Smits, and R. Helmig (2016), Effect of turbulence and roughness on coupled porous-medium/free-flow exchange processes, *Transp. Porous Med.*, *114*(2), 395–424, doi:10.1007/s11242-016-0654-6.
Fuchs, M., and A. Hadas (2011), Mulch resistance to water vapor transport, *Agric. Water Manage.*, *98*(6), 990–998, doi:10.1016/j.agwat.2011.01.008.
Gurr, C. G., T. J. Marshall, and J. T. Hutton (1952), Movement of water in soil due to a temperature gradient, *Soil Sci.*, *74*, 335–345.
Hadas, A. (1977), Evaluation of theoretically predicted thermal conductivities of soils under field and laboratory conditions, *Soil Sci. Soc. Am. J.*, *41*, 460–466, doi:10.2136/sssaj1977.03615995004100030006x.
Haghighi, E., E. Shahraeeni, P. Lehmann, and D. Or (2013), Evaporation rates across a convective air boundary layer are dominated by diffusion, *Water Resour. Res.*, *49*, 1602–1610, doi:10.1002/wrcr.20166.
Hahn, S., J. Je, and H. Choi (2002), Direct numerical simulation of turbulent channel flow with permeable walls, *J. Fluid Mech.*, *450*, 259–285, doi:10.1017/S0022112001006437.
Harbeck, G. E. (1962), A practical field technique for measuring reservoir evaporation utilizing mass-transfer theory, *U.S. Geol. Surv. Prof. Pap.*, *272E*, 101–105.
Ho, C. K., and S. W. Webb (1998), Review of porous media enhanced vapor-phase diffusion mechanisms, models, and data—Does enhanced vapor-phase diffusion exist?, *J. Porous Media*, *1*(1), 71–92, doi:10.1615/JPorMedia.v1.i1.60.
Hopmans, J. W., J. Simunek, and K. L. Bristow (2002), Indirect estimation of soil thermal properties and water flux using heat pulse probe measurements: Geometry and dispersion effects, *Water Resour. Res.*, *38*(1), 1006, doi:10.1029/2000WR000071.
Horton, R. (1989), Canopy shading effects on soil heat and water-flow, *Soil Sci. Soc. Am. J.*, *53*(3), 669–679doi:10.2136/sssaj1989.03615995005300030004x.
Ishihara, Y., E. Shimojima, and H. Harada (1992), Water-vapor transfer beneath bare soil where evaporation is influenced by a turbulent surface wind, *J. Hydrol.*, *131*(1–4), 63–104, doi:10.1016/0022-1694(92)90213-f.
Katata, G., H. Nagai, H. Ueda, N. Agam, and P. R. Berliner (2007), Development of a land surface model including evaporation and adsorption processes in the soil for the land-air exchange in arid regions, *J. Hydrometeorol.*, *8*(6), 1307–1324, doi:10.1175/2007JHM829.1.
Kimball, B. A., and E. R. Lemon (1971), Air turbulence effects upon soil gas exchange, *Soil Sci. Soc. Am. Proc.*, *35*(1), 16–21doi:10.2136/sssaj1971.03615995003500010013x.
Kondo, J., N. Saigusa, and T. Sato (1990), A parameterization of evaporation from bare soil surfaces, *J. Appl. Meteorol.*, *29*(5), 385–389, doi:10.1175/1520-0450(1990)029 < 0385:APOEFB>2.0.CO;2.
Lehmann, P., and D. Or (2009), Evaporation and capillary coupling across vertical textural contrasts in porous media, *Phys. Rev. E*, *80*(4), 046318, doi:10.1103/PhysRevE.80.046318.
Lehmann, P., I. Neuweiler, J. Vanderborght, and H. J. Vogel (2012), Dynamics of fluid interfaces and flow and transport across material interfaces in porous media: Modeling and observations, *Vadose Zone J.*, *11*(3), doi:10.2136/vzj2012.0105.
Li, H., F. Wu, H. Zhan, F. Qiu, and W. Wang (2016), The effect of precipitation pulses on evaporation of deeply buried phreatic water in extra-arid areas, *Vadose Zone J.*, *15*, doi:10.2136/vzj2015.09.0127.
Lu, S., T. S. Ren, Y. S. Gong, and R. Horton (2007), An improved model for predicting soil thermal conductivity from water content at room temperature, *Soil Sci. Soc. Am. J.*, *71*(1), 8–14, doi:10.2136/sssaj2006.0041.
Lu, S., T. Ren, Y. Gong, and R. Horton (2008), Evaluation of three models that describe soil water retention curves from saturation to oven dryness, *Soil Sci. Soc. Am. J.*, *72*(6), 1542–1546, doi:10.2136/sssaj2007.0307N.
Mahfouf, J. F., and J. Noilhan (1991), Comparative-study of various formulations of evaporation from bare soil using insitu data, *J. Appl. Meteorol.*, *30*(9), 1354–1365, doi:10.1175/1520-0450(1991)030 < 1354:CSOVFO>2.0.CO;2.
Maier, M., H. Schack-Kirchner, M. Aubinet, S. Goffi, B. Longdoz, and F. Parent (2012), Turbulence effect on gas transport in three contrasting forest soils, *Soil Sci. Soc. Am. J.*, *76*(5), 1518–1528, doi:10.2136/sssaj2011.0376.
Millington, R., and J. P. Quirk (1961), Permeability of porous solids, *Trans. Faraday Soc.*, *57*(8), 1200–1207doi:10.1039/TF9615701200.
Milly, P. C. D. (1982), Moisture and heat-transport in hysteretic, inhomogeneous porous-media—A matric head-based formulation and a numerical-model, *Water Resour. Res.*, *18*(3), 489–498, doi:10.1029/WR018i003p00489.
Milly, P. C. D. (1984), A simulation analysis of thermal effects on evaporation from soil, *Water Resour. Res.*, *20*(8), 1087–1098, doi:10.1029/WR020i008p01087.
Modaihsh, A. S., R. Horton, and D. Kirkham (1985), Soil-water evaporation suppression by sand mulches, *Soil Sci.*, *139*(4), 357–361.
Monteith, J. L., and M. H. Unsworth (1990), *Principles of Environmental Physics*, Edward Arnold, London.
Moret, D., I. Braud, and J. L. Arrue (2007), Water balance simulation of a dryland soil during fallow under conventional and conservation tillage in semiarid aragon, northeast spain, *Soil Tillage Res.*, *92*(1–2), 251–263, doi:10.1016/j.still.2006.03.012.
Mortensen, A. P., J. W. Hopmans, Y. Mori, and J. Simunek (2006), Multi-functional heat pulse probe measurements of coupled vadose zone flow and transport, *Adv. Water Resour.*, *29*(2), 250–267, doi:10.1016/j.advwatres.2005.03.017.
Mosthaf, K., K. Baber, B. Flemisch, R. Helmig, A. Leijnse, I. Rybak, and B. Wohlmuth (2011), A coupling concept for two-phase compositional porous-medium and single-phase compositional free flow, *Water Resour. Res.*, *47*, W10522, doi:10.1029/2011WR010685.
Mosthaf, K., R. Helmig, and D. Or (2014), Modeling and analysis of evaporation processes from porous media on the rev scale, *Water Resour. Res.*, *50*, 1059–1079, doi:10.1002/2013WR014442.
Nassar, I. N., and R. Horton (1997), Heat, water, and solute transfer in unsaturated porous media. 1: Theory development and transport coefficient evaluation, *Transp. Porous Med.*, *27*(1), 17–38, doi:10.1023/a:1006583918576.
Nassar, I. N., and R. Horton (1999), Salinity and compaction effects on soil water evaporation and water and solute distributions, *Soil Sci. Soc. Am. J.*, *63*(4), 752–758, doi:10.2136/sssaj1999.634752x.
Nieber, J. L., and M. F. Walter (1981), Two-dimensional soil-moisture flow in a sloping rectangular region—Experimental and numerical-studies, *Water Resour. Res.*, *17*(6), 1722–1730, doi:10.1029/WR017i006p01722.
Nimmo, J. R., and E. E. Miller (1986), The temperature-dependence of isothermal moisture vs potential characteristics of soils, *Soil Sci. Soc. Am. J.*, *50*(5), 1105–1113, doi:10.2136/sssaj1986.03615995005000050004x.
Noborio, K., K. J. McInnes, and J. L. Heilman (1996), Two-dimensional model for water, heat, and solute transport in furrow-irrigated soil. 2: Field evaluation, *Soil Sci. Soc. Am. J.*, *60*(4), 1010–1021, doi:10.2136/sssaj1996.03615995006000040008x.
Novak, M. D. (2010), Dynamics of the near-surface evaporation zone and corresponding effects on the surface energy balance of a drying bare soil, *Agric. For. Meteorol.*, *150*(10), 1358–1365, doi:10.1016/j.agrformet.2010.06.005.

Nuske, P., V. Joekar-Niasar, and R. Helmig (2014), Non-equilibrium in multiphase multicomponent flow in porous media: An evaporation example, *Int. J. Heat Mass Transfer*, *74*, 128–142, doi:10.1016/j.ijheatmasstransfer.2014.03.011.
Or, D., P. Lehmann, E. Shahraeeni, and N. Shokri (2013), Advances in soil evaporation physics—A review, *Vadose Zone J.*, *12*(4), doi:10.2136/vzj2012.0163.
Ouedraogo, F., F. Cherblanc, B. Naon, and J. C. Benet (2013), Water transfer in soil at low water content. Is the local equilibrium assumption still appropriate?, *J. Hydrol.*, *492*, 117–127, doi:10.1016/j.jhydrol.2013.04.004.
Peters, A., and W. Durner (2008), A simple model for describing hydraulic conductivity in unsaturated porous media accounting for film and capillary flow, *Water Resour. Res.*, *44*, W11417, doi:10.1029/2008WR007136.
Philip, J. R., and D. A. De Vries (1957), Moisture movement in porous materials under temperature gradients, *Trans. AGU*, *38*(2), 222–232, doi:10.1029/TR038i002p00222.
Potter, K. N., R. Horton, and R. M. Cruse (1987), Soil surface-roughness effects on radiation reflectance and soil heat-flux, *Soil Sci. Soc. Am. J.*, *51*(4), 855–860, doi:10.2136/sssaj1987.03615995005100040003x.
Poulsen, T. G., and P. Moldrup (2006), Evaluating effects of wind-induced pressure fluctuations on soil-atmosphere gas exchange at a landfill using stochastic modelling, *Waste Manage. Res.*, *24*(5), 473–481, doi:10.1177/0734242x06066363.
Reshetin, O. L., and S. Y. Orlov (1998), Theory of heat and moisture transfer in a capillary-porous body, *Tech. Phys.*, *43*(2), 263–264, doi:10.1134/1.1258982.
Rollins, R. L., M. G. Spangler, and D. Kirkham (1954), Movement of soil moisture under a thermal gradient, *Highway Res. Board Proc.*, *33*, 492–508.
Rose, C. W. (1967), Water transport in soil with a daily temperature wave. I: Theory and experiment, *Aust. J. Soil Res.*, *6*, 31–44.
Ruiz, T., and J. C. Benet (2001), Phase change in a heterogeneous medium: Comparison between the vaporisation of water and heptane in an unsaturated soil at two temperatures, *Transp. Porous Med.*, *44*(2), 337–353, doi:10.1023/a:1010773928372.
Saffman, P. G. (1971), Boundary condition at surface of a porous medium, *Stud. Appl. Math.*, *50*(2), 93–101, doi:10.1002/sapm197150293.
Saito, H., J. Simunek, and B. P. Mohanty (2006), Numerical analysis of coupled water, vapor, and heat transport in the vadose zone, *Vadose Zone J.*, *5*(2), 784–800, doi:10.2136/vzj2006.0007.
Sakai, M., S. B. Jones, and M. Tuller (2011), Numerical evaluation of subsurface soil water evaporation derived from sensible heat balance, *Water Resour. Res.*, *47*, W02547, doi:10.1029/2010WR009866.
Schlüter, S., H.-J. Vogel, O. Ippisch, P. Bastian, K. Roth, H. Schelle, W. Durner, R. Kasteel, and J. Vanderborght (2012), Virtual soils: Assessment of the effects of soil structure on the hydraulic behavior of cultivated soils, *Vadose Zone J.*, *11*(4), doi:10.2136/vzj2011.0174.
Schoups, G., J. W. Hopmans, C. A. Young, J. A. Vrugt, and W. W. Wallender (2005), Multi-criteria optimization of a regional spatially-distributed subsurface water flow model, *J. Hydrol.*, *311*(1–4), 20–48, doi:10.1016/j.jhydrol.2005.01.001.
Scotter, D. R., and P. A. C. Raats (1969), Dispersion of water vapor in soil due to air turbulence, *Soil Sci.*, *108*(3), 170–176, doi:10.1097/00010694-196909000-00004.
Seager, R., et al. (2007), Model projections of an imminent transition to a more arid climate in southwestern north america, *Science*, *316*(5828), 1181–1184, doi:10.1126/science.1139601.
Seneviratne, S. I., D. Lüthi, M. Litschi, and C. Schär (2006), Land-atmosphere coupling and climate change in europe, *Nature*, *443*(7108), 205–209, doi:10.1038/nature05095
Shahraeeni, E., and D. Or (2011), Thermo-evaporative fluxes from heterogeneous porous surfaces resolved by infrared thermography, *Water Resour. Res.*, *46*, W09511, doi:10.1029/2009WR008455.
Shahraeeni, E., and D. Or (2012), Pore scale mechanisms for enhanced vapor transport through partially saturated porous media, *Water Resour. Res.*, *48*, W05511, doi:10.1029/2011WR011036.
Shahraeeni, E., P. Lehmann, and D. Or (2012), Coupling of evaporative fluxes from drying porous surfaces with air boundary layer: Characteristics of evaporation from discrete pores, *Water Resour. Res.*, *48*, W09525, doi:10.1029/2012WR011857.
Shepherd, R., and R. J. Wiltshire (1995), An analytical approach to coupled heat and moisture transport in soil, *Transp. Porous Med.*, *20*(3), 281–304, doi:10.1007/BF01073177.
Shokri, N., P. Lehmann, and D. Or (2009), Critical evaluation of enhancement factors for vapor transport through unsaturated porous media, *Water Resour. Res.*, *45*, W10433, doi:10.1029/2009WR007769.
Shuttleworth, W. J. (2012), *Terrestrial Hydrometeorology*, Wiley-Blackwell, Chichester, U. K.
Sillon, J. F., G. Richard, and I. Cousin (2003), Tillage and traffic effects on soil hydraulic properties and evaporation, *Geoderma*, *116*(1–2), 29–46, doi:10.1016/s0016-7061(03)00092-2.
Simunek, J., M. Sejna, H. Saito, M. Sakai, and M. T. van Genuchten (2008), The hydrus-1d software package for simulating the movement of water, heat, and multiple solutes in variably saturated media, version 4.08, *Rep.*, 330 pp., Dep. of Environ. Sci., Univ. of Calif., Riverside, Calif.
Smits, K. M., A. Cihan, T. Sakaki, and T. H. Illangasekare (2011), Evaporation from soils under thermal boundary conditions: Experimental and modeling investigation to compare equilibrium- and nonequilibrium-based approaches, *Water Resour. Res.*, *47*, W05540, doi:10.1029/2010WR009533.
Smits, K. M., A. Cihan, T. Sakaki, S. E. Howington, J. F. Peters, and T. H. Illangasekare (2013), Soil moisture and thermal behavior in the vicinity of buried objects affecting remote sensing detection: Experimental and modeling investigation, *IEEE Trans. Geosci. Remote Sens.*, *51*(5), 2675–2688, doi:10.1109/tgrs.2012.2214485.
Sophocleous, M. (1979), Analysis of water and heat flow in unsaturated-saturated porous media, *Water Resour. Res.*, *15*(5), 1195–1206, doi:10.1029/WR015i005p01195.
Suzuki, M., and S. Maeda (1968), On the mechanism of drying granular beds: Mass transfer from discontinuous source, *J. Chem. Eng. Jpn.*, *1*(1), 26–31, doi:10.1252/jcej.1.26.
Tang, J. Y., and W. J. Riley (2013a), A new top boundary condition for modeling surface diffusive exchange of a generic volatile tracer: Theoretical analysis and application to soil evaporation, *Hydrol. Earth Syst. Sci.*, *17*(2), 873–893, doi:10.5194/hess-17-873-2013.
Tang, J. Y., and W. J. Riley (2013b), Impacts of a new bare-soil evaporation formulation on site, regional, and global surface energy and water budgets in clm4, *J. Adv. Model. Earth Syst.*, *5*(3), 558–571, doi:10.1002/jame.20034.
Tarara, J. M., and J. M. Ham (1999), Measuring sensible heat flux in plastic mulch culture with aerodynamic conductance sensors, *Agric. For. Meteorol.*, *95*(1), 1–13, doi:10.1016/s0168-1923(99)00021-0.
Tarnawski, V. R., W. H. Leong, and K. L. Bristow (2000), Developing a temperature-dependent kersten function for soil thermal conductivity, *Int. J. Energy Res.*, *24*(15), 1335–1350, doi:10.1002/1099-114X(200012)24:15 < 1335::AID-ER652 > 3.0.CO;2-X.
Taylor, S. A., and L. Cavazza (1954), The movement of soil moisture in response to temperature gradients, *Soil Sci. Soc. Am. Proc.*, *18*, 351–358.

Trautz, A. C., K. M. Smits, and A. Cihan (2015), Continuum-scale investigation of evaporation from bare soil under different boundary and initial conditions: An evaluation of nonequilibrium phase change, *Water Resour. Res.*, *51*, 7630–7648, doi:10.1002/2014WR016504.

Tuller, M., and D. Or (2001), Hydraulic conductivity of variably saturated porous media: Film and corner flow in angular pore space, *Water Resour. Res.*, *37*(5), 1257–1276, doi:10.1029/2000WR900328.

Unger, P. W., and D. K. Cassel (1991), Tillage implement disturbance effects on soil properties related to soil and water conservation—A literature-review, *Soil Tillage Res.*, *19*(4), 363–382, doi:10.1016/0167-1987(91)90113-C.

van Genuchten, M. T. (1980), A closed-form equation for predicting the hydraulic conductivity of unsaturated soils, *Soil Sci. Soc. Am. J.*, *44*(5), 892–898, doi:10.2136/sssaj1980.03615995004400050002x.

van de Griend, A. A., and M. Owe (1994), Bare soil surface-resistance to evaporation by vapor diffusion under semiarid conditions, *Water Resour. Res.*, *30*(2), 181–188, doi:10.1029/93WR02747.

Vereecken, H., M. Vanclooster, M. Swerts, and J. Diels (1991), Simulating water and nitrogen behavior in soils cropped with winter-wheat, *Fertil. Res.*, *27*(2–3), 233–243, doi:10.1007/BF01051130.

Verstraete, M. M., and S. A. Schwartz (1991), Desertification and global change, *Vegetatio*, *91*(1–2), 3–13, doi:10.1007/978-94-011-3264-0_1.

Wang, K. C., and R. E. Dickinson (2012), A review of global terrestrial evapotranspiration: Observation, modeling, climatology, and climatic variability, *Rev. Geophys.*, *50*, 1–54, doi:10.1029/2011RG000373.

Warren, A. (1996), Desertification., in *The Physical Geography of Africa*, edited by W. M. Adams, A. S. Goudie and A. R. Orme, pp. 342–355, Oxford Univ. Press, Oxford, U. K.

White, F. M. (1991), *Viscous Fluid Flow*, 614 pp., McGraw-Hill, New York.

Wieringa, J. (1993), Representative roughness parameters for homogeneous terrain, *Boundary Layer Meteorol.*, *63*(4), 323–363, doi:10.1007/BF00705357.

Wilcox, D. C. (2006), *Turbulence Modeling for CFD*, DCW Ind., Inc.

Xie, Z. K., Y. J. Wang, W. L. Jiang, and X. H. Wei (2006), Evaporation and evapotranspiration in a watermelon field mulched with gravel of different sizes in northwest china, *Agric. Water Manage.*, *81*(1–2), 173–184, doi:10.1016/j.agwat.2005.04.004.

Yamanaka, T., M. Inoue, and I. Kaihotsu (2004), Effects of gravel mulch on water vapor transfer above and below the soil surface, *Agric. Water Manage.*, *67*(2), 145–155, doi:10.1016/j.agwat.2004.01.002.

Yang, K., T. Koike, H. Ishikawa, J. Kim, X. Li, H. Z. Liu, S. M. Liu, Y. M. Ma, and J. M. Wang (2008), Turbulent flux transfer over bare-soil surfaces: Characteristics and parameterization, *J. Appl. Meteorol. Climatol.*, *47*(1), 276–290, doi:10.1175/2007jamc1547.1.

Yuan, C., T. Lei, L. Mao, H. Liu, and Y. Wu (2009), Soil surface evaporation processes under mulches of different sized gravel, *Catena*, *78*(2), 117–121, doi:10.1016/j.catena.2009.03.002.